

1 **Challenging age-related decline in brain function: Evidence from**
2 **fast neuroimaging of musical sequence recognition**
3

4 *Bonetti, L.^{1,2,3*}, Fernández Rubio, G.¹, Lumaca, M.¹, Carlomagno, F.^{1,4}, Risgaard Olsen, E.¹,*
5 *Criscuolo, A.⁵, Kotz, S.A.⁵, Vuust, P.¹, Brattico, E.^{1,4} & Kringelbach, M.L.^{1,2,3}*

6

7 ¹ *Center for Music in the Brain, Department of Clinical Medicine, Aarhus University & The Royal Academy of*
8 *Music, Aarhus, Aalborg, Denmark*

9 ² *Centre for Eudaimonia and Human Flourishing, Linacre College, University of Oxford, Oxford, United*
10 *Kingdom*

11 ³ *Department of Psychiatry, University of Oxford, Oxford, United Kingdom*

12 ⁴ *Department of Education, Psychology, Communication, University of Bari Aldo Moro, Italy*

13 ⁵ *Department of Neuropsychology and Psychopharmacology, Faculty of Psychology and Neuroscience,*
14 *Maastricht University, Maastricht, The Netherlands*

15

16

17

18

19 *Corresponding author: leonardo.bonetti@psych.ox.ac.uk

20

21 **Abstract**

22 Aging is often associated with decline in brain processing power and neural predictive
23 capabilities. To challenge this notion, we used the excellent temporal resolution of
24 magnetoencephalography (MEG) to record the whole-brain activity of 39 older adults (over
25 60 years old) and 37 young adults (aged 18-25 years) during recognition of previously
26 memorised and novel musical sequences. Our results demonstrate that independent of
27 behavioural measures, older compared to young adults showed increased rapid auditory
28 cortex responses (around 100 and 250 ms after each tone of the sequence) and decreased later
29 responses (around 250 and 350 ms) in hippocampus, ventromedial prefrontal cortex and
30 inferior frontal gyrus. Working memory abilities were associated with stronger brain activity
31 for both young and older adults. Our findings unpick the complexity of the healthy aging
32 brain, showing age-related neural transformations in predictive and memory processes and
33 challenging simplistic notions that non-pathological aging merely diminishes neural
34 predictive capabilities.

35

36 **Keywords**

37 Aging, Recognition memory, Temporal sequences, Predictive coding (PC),
38 Magnetoencephalography (MEG)

39 **Introduction**

40 Aging is a major omni comprehensive phenomenon which brings new challenges and places
41 large financial burden on society^{1, 2}. While most studies have investigated the biological
42 correlates of full-blown disorders such as Alzheimer's and other types of dementia^{3, 4}, less
43 research has focused on the neural changes associated with normal, non-pathological aging.
44 However, this is crucial to understand the modifications of the brain function and structure
45 across the lifespan and to eventually identify early markers of the age-related neural decline.

46 Previous research on the neurophysiology of non-pathological aging has predominantly
47 examined age-related changes in resting state brain activity⁵⁻⁸. This research has revealed
48 differences between the spontaneous brain functioning of young versus older adults. For
49 instance, in a magnetoencephalography (MEG) study, Tibon and colleagues⁵ reported that
50 decreased occurrence of lower-order and increased occurrence of higher-order brain networks
51 were linked to aging. Similarly, combining functional connectivity derived from MEG resting
52 state data with performance in motor learning, Mary and colleagues⁶ revealed that young and
53 older participants presented differently active neural circuits in resting state after being
54 exposed to motor learning. In another study, Alù and colleagues examined the impact of
55 aging on brain dynamics using electroencephalography (EEG) data and entropy analysis. The
56 findings revealed that older participants had overall higher entropy values across brain
57 regions compared to younger ones⁷. In another investigation using resting state EEG, the
58 authors found a decrease in occipital delta and posterior cortical alpha rhythms associated
59 with aging⁸.

60 Moving away from resting state, a few studies have investigated the impact of aging on
61 automatic brain processes such as the mismatch negativity (MMN), a component of the even-
62 related potential/field (ERP/F) which automatically originates in response to deviant stimuli⁹
63¹⁵. For instance, using MEG, Cheng and colleagues¹³ showed a reduction in the fronto-
64 temporo-parietal activity underlying MMN in older compared to young participants. In
65 another MEG study, the authors revealed that longer peak latencies and smaller amplitudes
66 were found in the MMN of older versus young adults¹⁴. Similarly, in an EEG study, Kisley
67 and colleagues showed that older adults presented reduced MMN amplitude at fronto-central
68 sites and decreased sensory gating efficiency compared to younger adults¹⁵. Taking together,
69 these findings suggest that aging is associated with declines in automatic central auditory
70 processing of deviant stimuli and with a mild decline of the cognitive ear, possibly related to
71 slow brain atrophy typical of aging¹⁶.

72 The neurophysiology of aging has also focused on memory task-based paradigms ¹⁷⁻²⁰. For
73 instance, a few studies suggested that the brain functioning during long-term recognition is
74 impaired in older compared to young adults. Gajewski and Falkenstein ¹⁷ revealed decreased
75 and delayed ERP components (e.g. N200, P300a and P300b) in older adults when they
76 performed a two-back memory task. Along this line, using EEG, Vaden and colleagues ¹⁸
77 showed that in a suppression of visual information task, the correct performances were
78 associated with a robust modulation of alpha power only in young but not in older adults.
79 Similarly, Federmeier and colleagues ¹⁹ demonstrated that older compared to young adults
80 had a reduced neural efficiency when recognising familiar words.

81 Previous research has also investigated the impact of aging on short-term recognition of
82 information, showing altered brain functioning in older compared to young adults. In a
83 classic MEG study, Babiloni and colleagues ²⁰ used two delayed response tasks, reporting
84 altered alpha event-related desynchronisation (ERD) associated with aging. In a recent EEG
85 study, Costa and colleagues ²¹ investigated the age-related differences in the neural activity
86 during short-term recognition of musical sequences. They showed that older adults reported
87 decreased slow negative responses associated with auditory processing compared to young
88 participants.

89 Taken together, the largest part of research on the neurophysiology of aging has
90 concentrated on resting state studies. Still, thorough examinations of the age-related neural
91 changes of memory have been produced, pointing to an overall impaired brain functioning in
92 older populations. However, little is known on the impact of aging on the fast-scale brain
93 dynamics underlying predictive and memory processes of sequences unfolding over time.
94 Similarly, the age-related neural changes underlying predictions in cognitive tasks remain
95 elusive.

96 To address these intriguing topics, the predictive coding theory (PCT) offers a suitable
97 framework. Indeed, PCT states that the brain is constantly updating internal models to predict
98 information and stimuli from the external world ²². In recent years, music has emerged as a
99 privileged tool to investigate PCT and understand how the brain encodes, recognises and
100 predicts temporal sequences ^{23, 24}. Along this line, in our previous studies we have combined
101 recently developed musical memory paradigms with state-of-the-art neuroimaging
102 techniques, focusing on the brain dynamics of healthy young participants when they encoded
103 and recognised musical sequences. We discovered that encoding of sounds recruited a large
104 network of functionally connected brain areas, especially in the right hemisphere, such as

105 Heschl's and superior temporal gyri, frontal operculum, cingulate gyrus, insula, basal ganglia,
106 and hippocampus ²⁵. Similarly, long-term recognition of short musical sequences recruited
107 nearly the same brain network. However, in this case, the recruitment was bilateral, and it
108 showed hierarchical dynamics from lower- to higher-order brain areas in different frequency
109 bands (e.g. 0.1-1 Hz and 2-8 Hz) ²⁶ and in relation to the recognition of previously
110 memorised or varied musical sequences ²⁷⁻³⁰.

111 In the current study, we took a new fundamental step by using musical memory paradigms
112 and advanced neuroimaging techniques to investigate the impact of aging on the fast-scale
113 brain dynamics underlying predictive and memory processes for musical sequences unfolding
114 over time.

115

116 **Results**

117 **Overview of the experimental design and analysis pipeline**

118 In this study, we investigated the impact of aging on the fast-scale spatiotemporal brain
119 dynamics underlying recognition of previously memorised musical sequences. In brief,
120 during magnetoencephalography (MEG) recordings, two groups of participants (39 older
121 adults [older than 60 years old] and 37 young adults [younger than 25 years old]) listened to
122 the first musical sentence of the Prelude in C minor, BWV 847 by Johann Sebastian Bach and
123 were instructed to memorise it to the best of their ability. As shown in **Figure 1** and **Figure**
124 **S1**, participants were subsequently presented with five-tone musical excerpts (M) taken from
125 the music they previously memorised and with carefully matched variations. The variations
126 consisted of five-tone musical sequences generated by systematically altering the M
127 sequences after either the first (NT1) or third (NT3) tone. For each musical sequence,
128 participants were requested to assess whether the sequence was taken from the memorised
129 musical piece (M) or whether it was new (N). Additional details on the stimuli are available
130 in the Methods section. Key background information on the two samples of participants is
131 reported in **Table 1**.

132 The analysis pipeline of this study is partly depicted in **Figure 1** and consisted of
133 contrasting the brain activity of young versus older adults at MEG sensor and source levels.

134 First, we used Monte Carlo simulations (MCS) on univariate tests of MEG sensor data.
135 This was followed by estimating the sources of the brain activity which generated the
136 differences between young and older adults. Second, we focused on eight key regions of
137 interest (ROIs) and analysed whether their time series differed between older and young
138 adults. Third, we assessed the impact of WM, years of general and musical education, sex,
139 and age groups on the brain activity underlying recognition of the musical sequences.

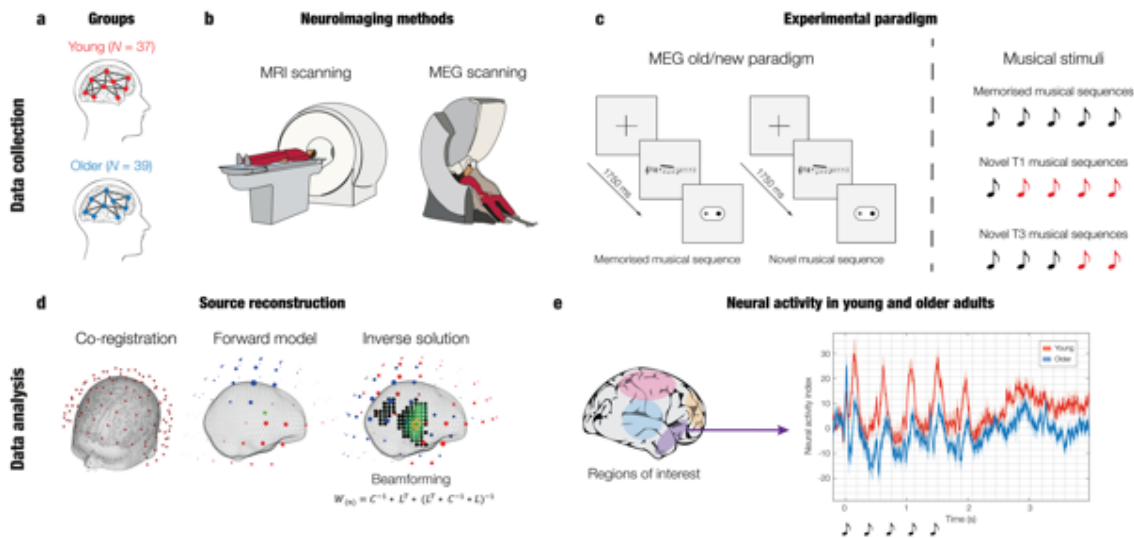
140 Additional details are available in the Methods section, while the codes used for these
141 analyses are extensively reported at the following links:

142 https://github.com/leonardob92/MEG_Aging_Bach.git

143 <https://github.com/leonardob92/LBPD-1.0.git>

144

145



146
147

148 **Figure 1. Experimental design, stimuli, and analysis pipeline.**

149 **a** – Thirty-seven young and 39 older adults were invited to participate in the experiment. **b** – The brain activity
150 of the participants was collected using magnetoencephalography (MEG), while their structural brain images
151 were acquired using magnetic resonance imaging (MRI). **c** – Participants were requested to memorise a short
152 musical piece (lasting about 30 seconds). Then, we used an old/new auditory recognition task (left). Here, one
153 at a time, five-tone temporal sequences (i.e., musical melodies) were presented in randomised order and
154 participants were instructed to respond with button presses whether they were taken from the musical piece they
155 previously memorised ('old' or memorised musical sequences, 'M') or they were novel ('new' musical
156 sequences, 'N'). Three types of temporal sequences (M, NT1, NT3) were used in the study. The figure shows a
157 graphical depiction of how the novel musical sequences were created with regards to the previously memorised
158 ones (right). The N sequences were created through systematic variations of the M sequences. For example, in
159 the middle row, it is depicted a sequence (NT1) where we changed all tones but the first one (indicated by the
160 red colours). Likewise, the bottom row shows a sequence where we changed only the last two tones (NT3). **c** –
161 After pre-processing the MEG data, we co-registered it with the individual anatomical MRI data and
162 reconstructed its brain sources using a beamforming algorithm. This procedure returned one time series for
163 each of the 3559 reconstructed brain sources. **e** – We constrained the source reconstructed data to eight brain
164 regions of interest (ROIs) which were selected based on previous literature (left). For each of the ROI, we
165 studied the differences over time between the brain activity of young versus older adults (right).

166
167
168
169
170
171

Participant groups	N	Age	Sex	WM (raw)	Musical training (years)	Education (years)
Young adults (< 25)	37	21.89 ± 2.05	18 F; 19 M	43.00 ± 7.15	3.24 ± 3.72	13.57 ± 2.62
Older adults (> 60)	39	67.72 ± 5.35	24 F; 15 M	38.42 ± 7.71	3.08 ± 4.31	14.20 ± 4.63

172

173 **Table 1. Background information on the two age samples**

174 Number of participants, age, sex, WM, years of musical training and general education reported independently
175 for the two age groups. The numbers for age, WM, and years of musical training and general education
176 correspond to mean and standard deviations.

177

178

179 **Behavioural results**

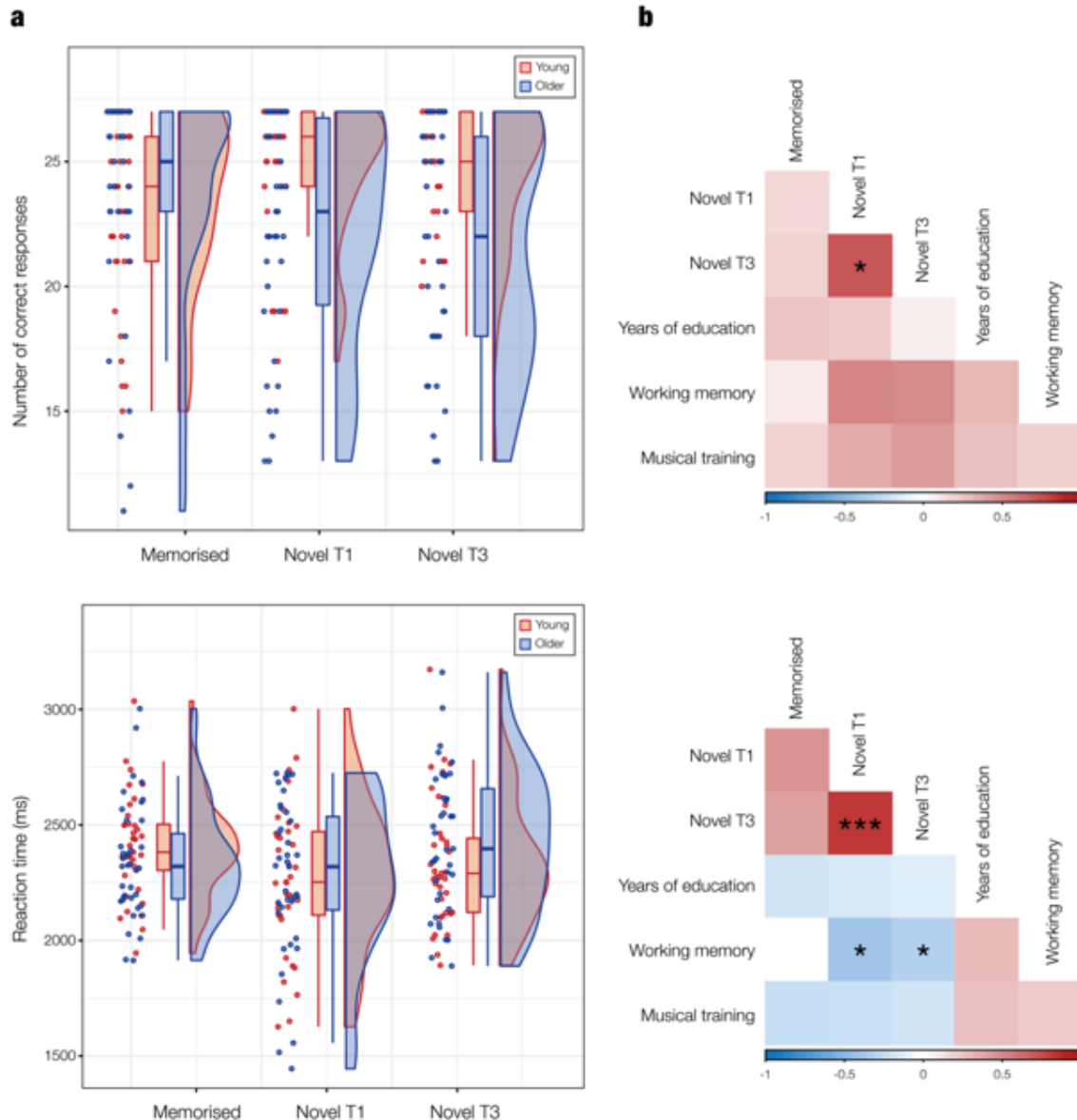
180 We calculated the impact of age on response accuracy and reaction times during the musical
181 recognition task that participants performed in the MEG.

182 Regarding the response accuracy, there was a statistically significant difference
183 between the two age groups in the memory task ($F(3, 61) = 7.18, p < .001$, Wilks' $\Lambda = .739$,
184 partial $\eta^2 = .26$). Follow-up ANCOVAs showed that older adults scored lower than young
185 adults when correctly identifying NT1 ($F(1, 63) = 13.03, p < .001$) and NT3 sequences ($F(1,$
186 $63) = 19.89, p < .001$). Years of education ($F(3, 61) = 3.37, p = .02$, Wilks' $\Lambda = .857$, partial
187 $\eta^2 = .14$), WM scores ($F(3, 61) = 7.07, p < .001$, Wilks' $\Lambda = .742$, partial $\eta^2 = .26$), and years
188 of musical training ($F(3, 61) = 4.61, p = .005$, Wilks' $\Lambda = .815$, partial $\eta^2 = .18$) were
189 statistically significant covariates. Specifically, years of education had a statistically
190 significant effect on correctly identifying M ($F(1, 63) = 4.58, p = .03$) and NT1 sequences
191 ($F(1, 63) = 6.52, p = .01$), meaning that higher number of years of education was associated
192 to higher number of correct responses. Similarly, WM capacity had a statistically significant
193 positive effect on correctly identifying NT1 ($F(1, 63) = 14.31, p < .001$) and NT3 sequences
194 ($F(1, 63) = 19.24, p < .001$). Finally, years of musical training had a statistically significant
195 positive effect on correctly identifying NT1 ($F(1, 63) = 5.45, p = .02$) and NT3 sequences
196 ($F(1, 63) = 13.80, p < .001$).

197 With respect to the average reaction time during recognition of M, NT1 and NT3
198 sequences, we found a statistically significant difference between the two age groups on the
199 reaction times ($F(3, 64) = 2.904, p = .04$, Wilks' $\Lambda = .880$, partial $\eta^2 = .12$). However, this
200 effect was non-significant in follow-up ANCOVAs. Regarding the covariates, only WM

201 scores had a significant effect on the dependent variables ($F(3, 64) = 5.18, p = .002$, Wilks' Λ
202 = .804, partial $\eta^2 = .20$). In particular, we observed that high WM scores were associated with
203 lower average reaction time when correctly identifying NT1 ($F(1, 66) = 10.96, p = .001$) and
204 NT3 sequences ($F(1, 66) = 4.29, p = .04$).

205



207

209 *Figure 2. Impact of aging, education, musical training and WM on the recognition of musical sequences.*

a – Raincloud plots show the overlapping distributions and normalized data points of both age groups with regards to the recognition of the previously memorised and novel (NT1 and NT3) musical sequences. Boxplots show the median and interquartile (IQR, 25 – 75%) range, whiskers depict the 1.5*IQR from the quartile. Each

213 dot corresponds to the number of correct responses (top plot) or the mean reaction time (bottom plot) of each
214 participant. The plot above refers to the number accuracy in the task, while the bottom plot to the reaction
215 times. **b** – Correlation matrix between memorised, NT1, NT3 (number of correct responses, top plot, and
216 reaction times, bottom plot), years of education, WM, years of musical training. Significant correlations are
217 indicated by the stars (* $p < .05$; ** $p < .01$; *** $p < .001$).

218

219

220 **Aging and whole-brain activity**

221 To assess the difference between the brain activity of older and young adults while they
222 recognised the musical sequences, we calculated several independent samples t-tests with
223 unequal variances and then corrected for multiple comparisons using cluster-based MCS (t-
224 test threshold = .05, MCS threshold = .001, 1000 permutations). As reported in detail in the
225 Methods section, this procedure was computed independently for the three experimental
226 conditions (M, NT1, NT3).

227 The analyses returned several significant clusters, highlighting overall reduced brain
228 activity along a wide array of MEG sensors in older participants. In addition, a few
229 significant clusters showed stronger brain activity in older participants. **Table 2** shows the
230 key information of the larger significant clusters for the three experimental conditions, while
231 **Table S1** provides complete statistical information.

232

233

Memorised musical sequences – young > older adults					
<i>Cluster #</i>	<i>Size</i>	<i>MCS p-val</i>	<i>Max t-val</i>	<i>Time (1)</i>	<i>Time (end)</i>
1	305	< .001	4,05	1,704	1,812
2	218	< .001	3,85	0,568	0,656
3	190	< .001	3,34	0,356	0,476

Memorised musical sequences – older > young adults					
<i>Cluster #</i>	<i>Size</i>	<i>MCS p-val</i>	<i>Max t-val</i>	<i>Time (1)</i>	<i>Time (end)</i>
1	292	< .001	-6,08	0,072	0,128

NT1 musical sequences – young > older adults					
<i>Cluster #</i>	<i>Size</i>	<i>MCS p-val</i>	<i>Max t-val</i>	<i>Time (1)</i>	<i>Time (end)</i>
1	415	< .001	4,47	0,272	0,400
2	215	< .001	4,10	1,760	1,908
3	175	< .001	4,85	1,916	1,996

NT1 musical sequences – older > young adults					
<i>Cluster #</i>	<i>Size</i>	<i>MCS p-val</i>	<i>Max t-val</i>	<i>Time (1)</i>	<i>Time (end)</i>
1	695	< .001	-7,03	0,048	0,164

NT3 musical sequences – young > older adults					
--	--	--	--	--	--

Cluster #	Size	MCS p-val	Max t-val	Time (1)	Time (end)
1	154	< .001	4, 26	1,292	1,420
2	88	< .001	4, 16	1,056	1,092
3	75	< .001	4, 16	1,068	1,140
NT3 musical sequences – older > young adults					
Cluster #	Size	MCS p-val	Max t-val	Time (1)	Time (end)
1	388	< .001	-5,43	0,076	0,144

234

235 **Table 2. The effect of aging on the whole-brain activity – MEG sensors**

236 *Information on the significant clusters emerged at MEG sensors level by contrasting the brain activity*
237 *underlying recognition of musical sequences of young versus older adults. The results are reported*
238 *independently for each condition (M, NT1, and NT3) and strength of the contrast (young > older and older >*
239 *young). The table shows the size of the cluster, the MCS p-value, the maximum t-value within the cluster and the*
240 *time extent of the significance of the difference between older and young adults.*

241

242

243 After analysing the brain activity at the MEG sensor level, we computed source
244 reconstruction analyses using a beamforming algorithm to estimate the brain sources that
245 generated the signal recorded by the MEG sensors. For each of the significant clusters, we
246 contrasted the source-reconstructed brain activity of older versus young adults and corrected
247 for multiple comparisons using a three-dimensional (3D) cluster-based MCS ($\alpha < .05$, MCS
248 p -value = .001). These analyses returned several significant clusters of brain activity,
249 revealing that the main brain regions differentiating older from young adults were the
250 primary and secondary auditory cortices, post-central gyrus, hippocampal regions, inferior
251 frontal gyrus, and ventromedial prefrontal cortex. These results are depicted in **Figures S3**
252 and **S4** and reported in detail in **Table S2** and **S3**.

253

254 **Aging and functional brain regions of interest (ROIs)**

255 To strengthen the reliability of our results and allow an easier comparison with previous
256 literature, we computed a complementary analysis by investigating the difference between the
257 brain activity of older versus young adults in a selected array of functional ROIs that were
258 previously described by Bonetti and colleagues ²⁸. These areas (described in detail in **Table**
259 **S4** and shown in **Figure S2**) were the bilateral medial cingulate gyrus (MC), bilateral
260 ventromedial prefrontal cortex (VMPFC), left (HITL) and right hippocampal area and
261 inferior temporal cortex (HITR), left (ACL) and right auditory cortex (ACR), and left (IFGL)
262 and right inferior frontal gyrus (IFGR). We contrasted the brain activity of young versus

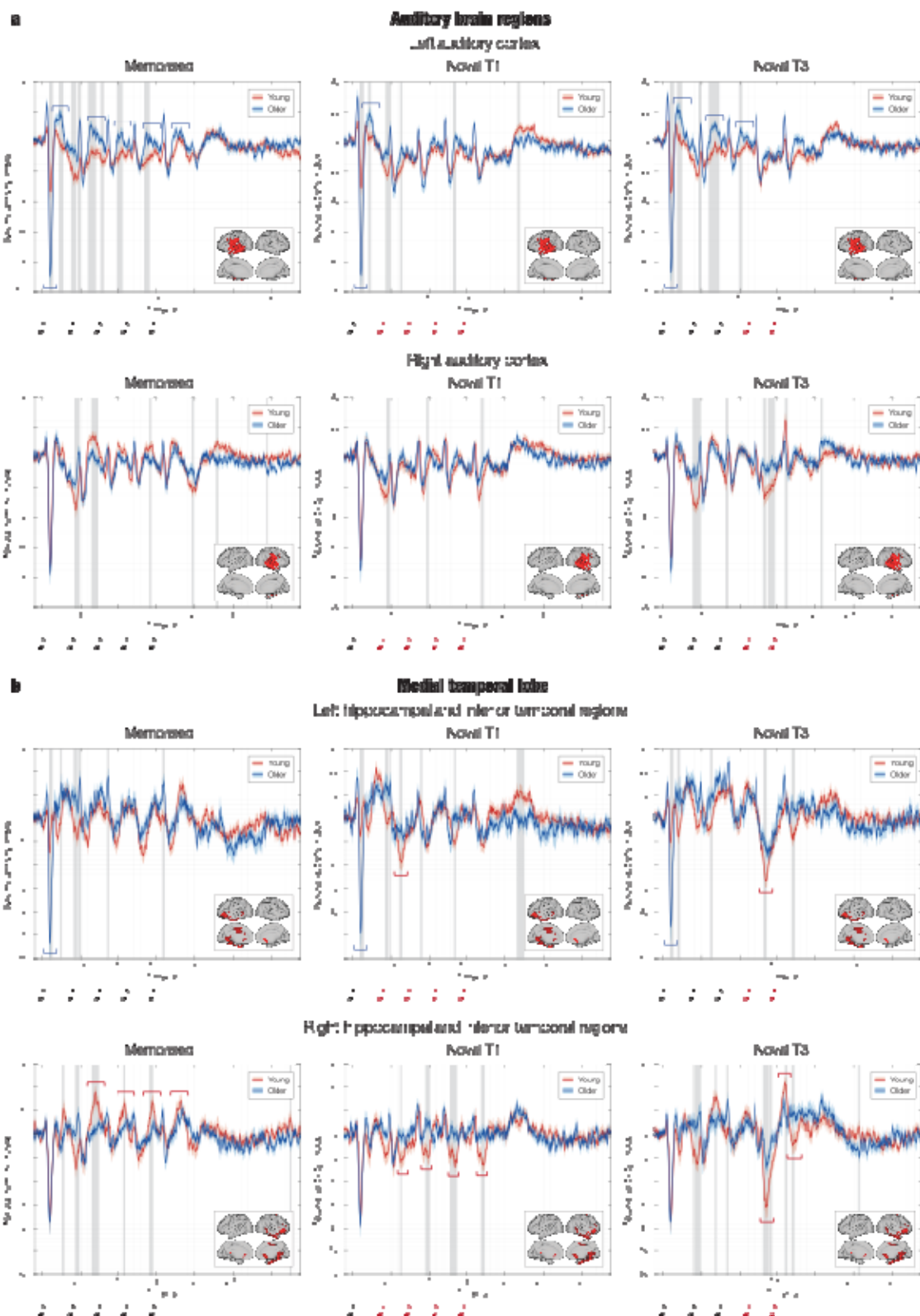
263 older adults by computing an independent-sample t-test for each ROI, timepoint, and
264 condition. We corrected for multiple comparisons using 1D cluster-based MCS (t-value
265 threshold = .05, MCS *p*-value = .001).

266 This analysis returned several significant clusters showing differences in the brain activity
267 of older compared to young adults. Of particular interest are the clusters reported in the HITR
268 (*p* < .001, *k* = 25; max *t-val* = 4.70, time: 640 – 736 ms) and IFGR (cluster 1: *p* < .001, *k* =
269 38; max *t-val* = -4.59, time: 464 – 612 ms; cluster 2: *p* < .001, *k* = 33; max *t-val* = -5.04, time:
270 1260 – 1388 ms) showing reduced activity for older versus young adults when recognising
271 previously memorised musical sequences. In addition, older versus young participants were
272 characterised by a weaker signal in response to the variation of the original musical
273 sequences. This was particularly evident for HITR (NT1: *p* < .001, *k* = 24; max *t-val* = -3.53,
274 time: 1284 – 1376 ms; NT3: *p* < .001, *k* = 21; max *t-val* = -4.01, time: 1320 – 1400 ms),
275 VMPFC (NT1: *p* < .001, *k* = 15; max *t-val* = -3.57, time: 1320 – 1376 ms; NT3: *p* < .001, *k* =
276 23; max *t-val* = -3.97, time: 1672 – 1760 ms), and HITL (NT3: *p* < .001, *k* = 12; max *t-val* = -
277 3.31, time: 1324 – 1368 ms).

278 Finally, older adults showed a stronger activity in ACL in response to the first tone of the
279 sequences in all conditions (M: *p* < .001, *k* = 14; max *t-val* = 5.37, time: 84 – 136 ms; NT1: *p*
280 < .001, *k* = 15; max *t-val* = 5.86, time: 88 – 144 ms; NT3: *p* < .001, *k* = 16; max *t-val* = 6.04,
281 time: 84 – 144 ms) and in relation to each tone until the variation was introduced (**Figure 3**,
282 first row). These results are depicted in **Figures 3** and **4** and extensively reported in **Table**
283 **S5**.

284

285



288 **Figure 3. Older adults show stronger activity in auditory cortex and reduced responses in medial temporal**
289 **lobe during recognition of musical sequences.**

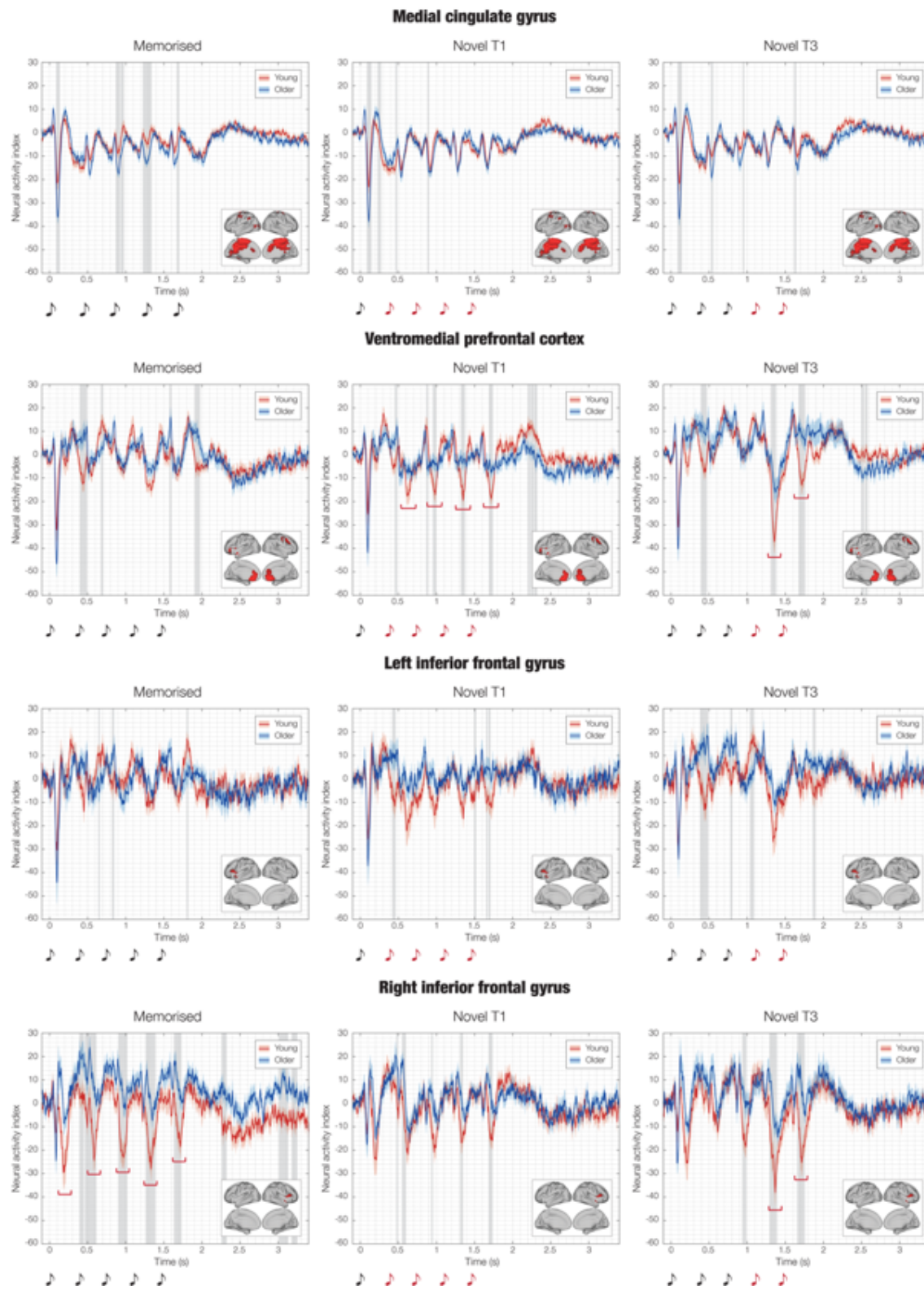
290 **a** - The results show that the older adults have significantly stronger activity in the left auditory cortex
291 compared to young adults only when recognising the melodies that were previously memorised. In fact, the top
292 graphs indicate a component occurring about 300 ms after the onset of each tone that was stronger for the older
293 adults for all the tones in the M condition and for all the tones before introducing the variations in the N
294 conditions (i.e. one tone for NT1 and three tones for NT3). In addition, the N100 response to the first tone of the
295 sequences was significantly stronger for old versus young adults in all conditions. **b** - Conversely, older adults
296 showed significantly decreased activity in the hippocampal and inferior temporal regions. This was particularly
297 evident for conditions NT1 and NT3. Here, as highlighted by the red bottom graphs, the older versus young
298 adults exhibited reduced prediction error responses when the sequence was varied. This happened especially
299 for the first tone which introduced the variation in the melodies (i.e. tone two for NT1 and tone four for NT3).
300 Finally, even if to a smaller extent, reduced activity in older adults was also observed for the M condition,
301 where positive components of the neural signals were reduced for all the tones except for the first one.

302 Note that the figure shows the source localised brain activity illustrated for each experimental condition (M,
303 NT1, NT3) in four ROIs (left and right auditory cortex, left and right hippocampal and inferior temporal
304 regions). Grey areas show the statistically significant differences of the brain activity between young (solid red
305 line) and older adults (solid blue, shading indicates standard error in both cases), while red and blue graphs
306 highlight neural components of particular interest. The sketch of the musical tones represents the onset of the
307 sounds forming the musical sequences. The brain templates illustrate the spatial extent of the ROIs.

308

309

310



311

312

313 **Figure 4. Impact of aging on the cingulate gyrus, ventromedial prefrontal cortex and inferior frontal gyrus**
314 **responses during recognition of musical sequences.**

315 The red graphs in the second row highlight that the VMPFC produced a weaker activity indexing prediction
316 error for the older versus young adults for conditions NT1 and NT3, in an analogous manner to the right
317 hippocampal and inferior temporal regions shown in **Figure 3**. Notably, while these two brain regions also
318 showed a decreased activity for the M condition for older versus young adults, this did not happen for the
319 VMPFC. Finally, the last row of this figure shows a much stronger activity originated in the right inferior
320 frontal gyrus of the young versus older adults. This was particularly evident for the M sequences and consisted
321 of a negative component peaking approximately 250 ms after the onset of each musical tone.

322 Note that the figure shows the source localised brain activity illustrated for each experimental condition (M,
323 NT1, NT3) in four ROIs (medial cingulate gyrus, ventromedial prefrontal cortex [VMPFC], left and right
324 inferior frontal gyrus). Grey areas show the statistically significant differences of the brain activity between
325 young (solid red line) and older adults (solid blue, shading indicates standard error in both cases), while red
326 and blue graphs highlight neural components of particular interest. The sketch of the musical tones represents
327 the onset of the sounds forming the musical sequences. The brain templates illustrate the spatial extent of the
328 ROIs.

329

330

331 **WM, musical expertise, education level, aging and neural data**

332 Finally, we computed two additional analyses to assess whether potential confounding
333 variables had an impact on the relationship between aging and the neural mechanisms
334 underlying recognition of musical sequences.

335 In the first analysis we computed three independent multivariate analyses of covariance
336 (MANCOVAs), one for each experimental condition. In each MANCOVA, the dependent
337 variables were the highest peaks of the neural data for the eight ROIs, while the independent
338 variables were age, sex, years of formal musical expertise, WM, and years of formal
339 education (see Methods for additional details).

340 The results of the MANCOVAs showed a significant main effect for age in all
341 experimental conditions: M ($F(8, 59) = 4.62, p = .0002$, Wilks' $\Lambda = .614$, partial $\eta^2 = .39$),
342 NT1 ($F(8, 59) = 3.117, p = .005$, Wilks' $\Lambda = .703$, partial $\eta^2 = .30$), and NT3 ($F(8, 59) =$
343 $3.575, p = .002$, Wilks' $\Lambda = .674$, partial $\eta^2 = .33$). This confirmed the impact of age on the
344 neural data. The other variables did not show any significant results, indicating that no
345 confounding variables affected the relationship between age and the neural data. However,
346 WM approached the significance in all experimental conditions, showing moderate effect
347 sizes: M ($F(8, 59) = 4.62, p = .09$, Wilks' $\Lambda = .802$, partial $\eta^2 = .20$), NT1 ($F(8, 59) =$
348 $1.313, p = .25$, Wilks' $\Lambda = .849$, partial $\eta^2 = .15$), and NT3 ($F(8, 59) = 1.691, p = .11$, Wilks'

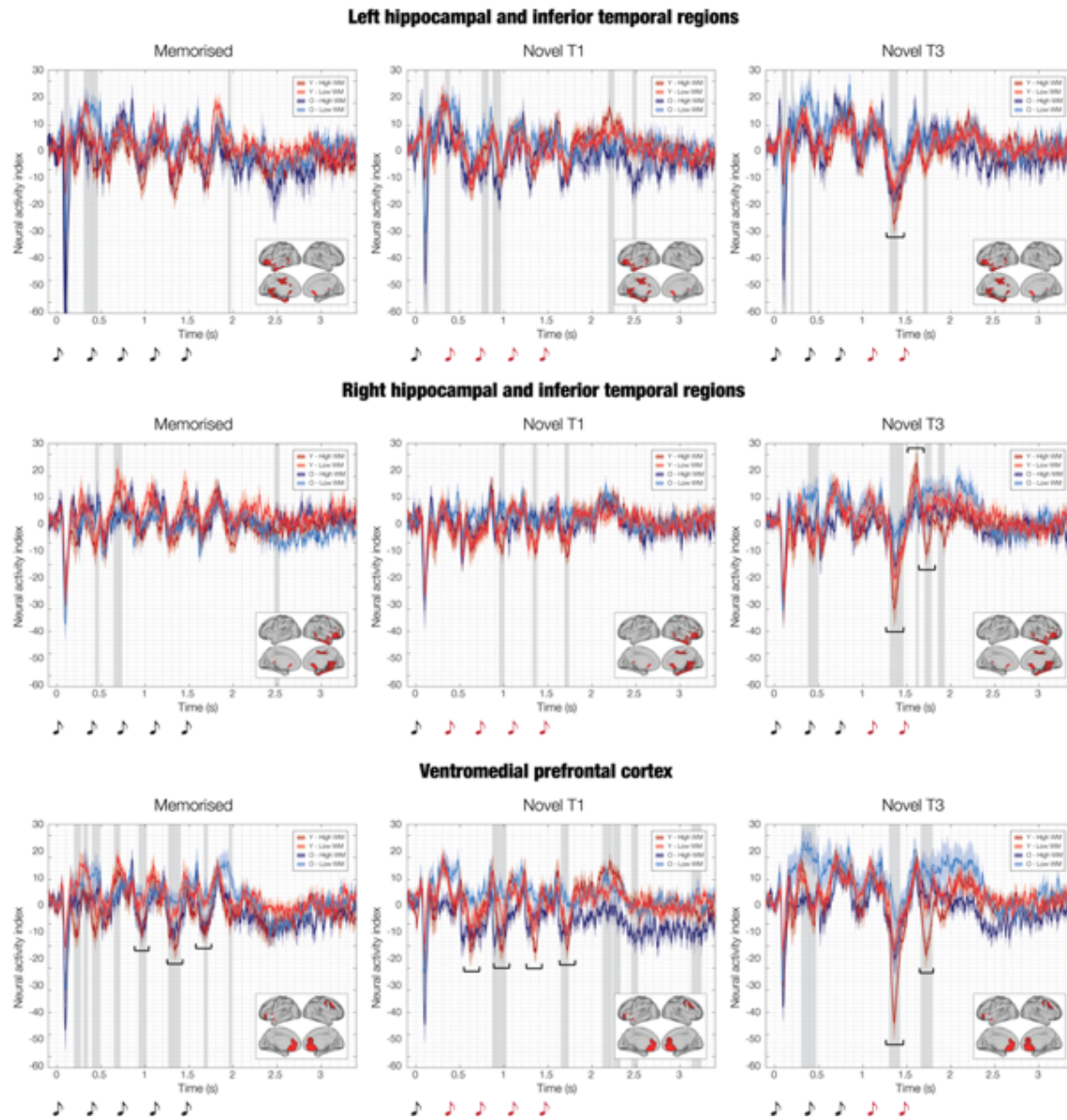
349 $\Lambda = .814$, partial $\eta^2 = .19$). This indicated that WM may partially affect the brain dynamics of
350 musical recognition in relation to aging.

351 Following the results of the MANCOVAs, we computed independent analyses of variance
352 (ANOVAs) for each time-point, ROI and condition and used cluster-based 3D MCS to
353 correct for multiple comparisons. We used two-way ANOVAs with the following levels:
354 WM (high and low performers) and age (older and young adults). The analysis returned
355 significant key clusters for three main ROIs in the NT3 condition: HITR (NT3: $p < .001$, $k =$
356 40; max $F\text{-val} = 17.66$, time: 1308 - 1464 ms), VMPPFC (NT3: $p < .001$, $k = 32$; max $F\text{-val} =$
357 13.57, time: 1300 - 1424 ms), HITL (NT3: $p < .001$, $k = 24$; max $F\text{-val} = 9.36$, time: 1304 -
358 1396 ms). **Figure 5** show the time series of these ROIs in relation to age and WM, while
359 detailed statistical results are reported in **Table S6**.

360

361

362



363

364

365 **Figure 5. Impact of WM and aging on the ventromedial prefrontal cortex and medial temporal lobe**
 366 **responses during recognition of musical sequences.**

367 The black graphs in the NT3 plots (all rows) highlight that the strongest brain prediction error in response to
 368 the variation of the original musical sequences occurred in young adults who performed very well in the WM
 369 tasks. The strength of the prediction error was lower and very similar for young adults with low WM and older
 370 adults with high WM. Finally, older adults with low WM presented the most reduced prediction error signal in
 371 the brain. This was particularly evident for the right hippocampal and inferior temporal regions as well as for
 372 the VMPFC. A similar, but less pronounced, effect was observed in the VMPFC for M and NT1.

373

374

375 Note that the figure shows the source localised brain activity illustrated for each experimental condition (M,
376 NT1, NT3) in three (ventromedial prefrontal cortex [VMPFC], left and right hippocampal and inferior temporal
377 regions). Graphs indicates the key event of interest in the brain responses, while the grey areas show the
378 statistically significant differences of the brain activity between the participants grouped in the following four
379 groups: young adults - high WM (i), young adults - low WM, older adults - high WM, older adults - low WM.
380 Solid line indicates the average over participants, independently for the four groups, while the shaded area the
381 standard errors. The sketch of the musical tones represents the onset of the sounds forming the musical
382 sequences. The brain templates illustrate the spatial extent of the ROIs.

383

384

385

386 Finally, we computed an additional sub-analysis to assess whether we could distinguish a
387 sub-sample of the older participants based on their brain activity. To this aim, we used one-
388 way ANOVAs contrasting three age-groups: young (younger than 25), older adults 60-68
389 (age between 60 and 68, n = 23) and older adults > 68 (older than 68, n = 16). Then, we
390 corrected for multiple comparisons with cluster-based 3D MCS. The results highlighted that
391 the oldest group within the older adults was characterised by overall reduced brain activity,
392 especially in response to the variation of the original sequences. This was particularly evident
393 for HITR (NT3: $p < .001$, $k = 22$; max $F\text{-val} = 7.92$, time: 1312 - 1396 ms), VMPFC (NT3: p
394 $< .001$, $k = 15$; max $F\text{-val} = 7.73$, time: 1320 - 1376 ms), HITL (NT3: $p < .001$, $k = 13$; max
395 $F\text{-val} = 10.01$, time: 1316 - 1364 ms). **Figure 6** shows the time series of these ROIs in
396 relation to the three age groups, while detailed statistical results are reported in **Table S7**.

397

398

399

400

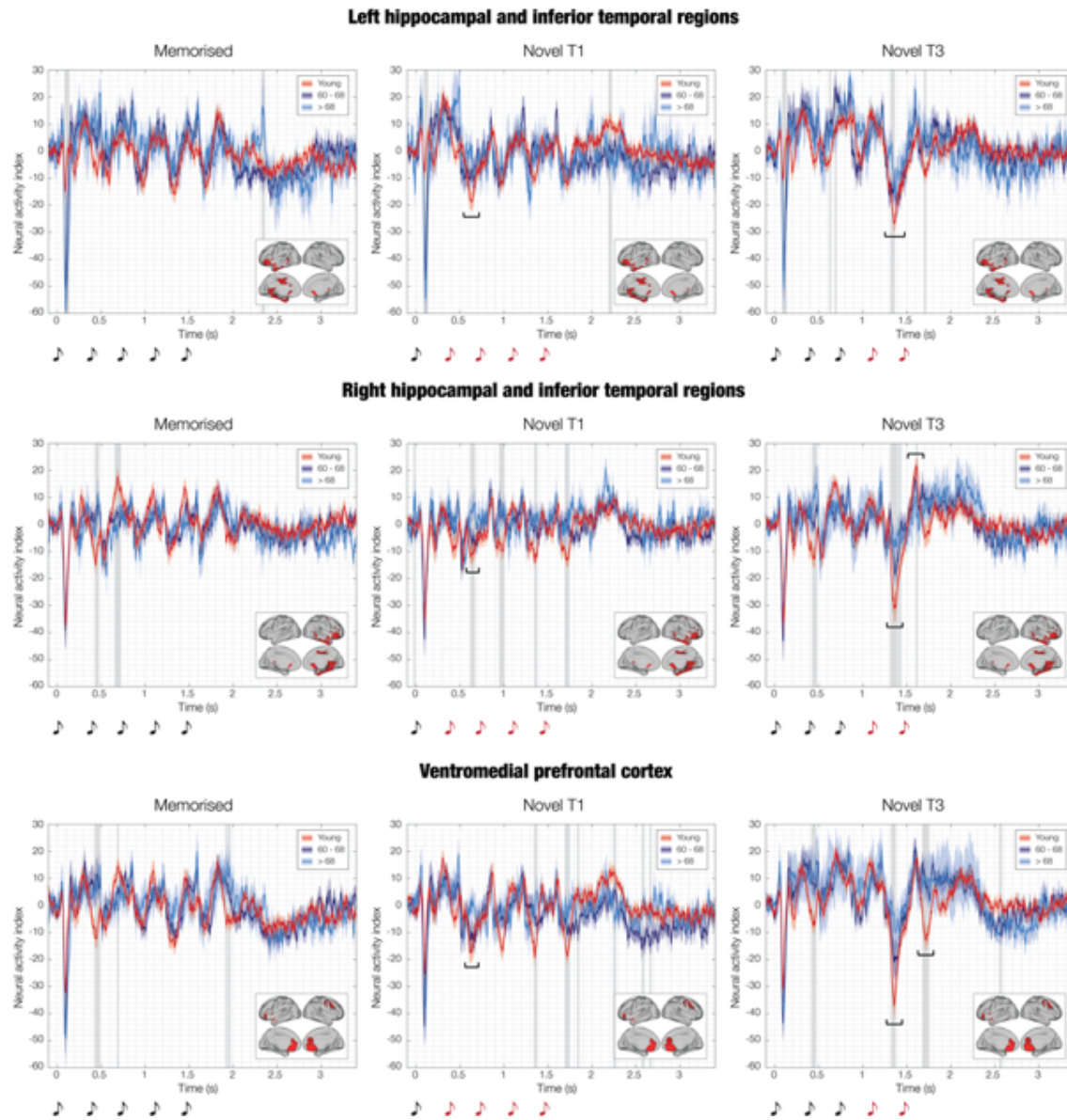


Figure 6. Ventromedial prefrontal cortex and medial temporal lobe responses during recognition of musical sequences for three age groups (young adults, adults between 60 and 68 years of age, adults older than 68).

The black graphs in the NT1 and NT3 plots (all rows) highlight that the strength of the brain prediction error in response to the variation of the original musical sequences was modulated by age. In fact, the strongest signal was recorded for the young adults. A reduced prediction error was observed for the adults aged between 60 and 68, while the weakest signal occurred for the adults older than 68 years. As observed for the WM in **Figure 5**, this effect was particularly evident for the VMPFC and right hippocampal and inferior temporal regions.

Note that the figure shows the source localised brain activity illustrated for each experimental condition (M, NT1, NT3) in three (ventromedial prefrontal cortex [VMPFC], left and right hippocampal and inferior temporal regions). Graphs indicates the key event of interest in the brain responses, while the grey areas show the statistically significant differences of the brain activity between the participants grouped in the following three

414 *groups: young adults (i), adults between 60 and 68 years of age (ii), adults older than 68 years (iii). Solid line*
415 *indicates the average over participants, independently for the four groups, while the shaded area the standard*
416 *errors. The sketch of the musical tones represents the onset of the sounds forming the musical sequences. The*
417 *brain templates illustrate the spatial extent of the ROIs.*

418

419

420

421

422

423

424 **Discussion**

425 In this study, we have combined fast neuroimaging with the recognition of previously
426 memorised and novel musical sequences to unpick the complexity of the healthy aging brain.
427 Our findings challenge simplistic notions that non-pathological aging merely diminishes
428 neural predictive capabilities by showing age-related neural transformations in predictive and
429 memory processes.

430 During the recognition of the previously memorised melodies, the left auditory cortex
431 exhibited stronger activity in response to each sound of the sequence for the older compared
432 to young adults. Conversely, other brain regions of key importance for memory and
433 predictive processes such as the hippocampus, inferior temporal cortex and inferior frontal
434 gyrus showed an overall decreased activity for the older adults. In response to the varied
435 musical sequences, the left auditory cortex did not exhibit any difference between older and
436 young adults after the musical sequence was altered. Conversely, a much-reduced activity
437 was observed for the older adults after the sequence was changed. This effect was particularly
438 strong for the condition NT3 where the sequence was altered after the fourth tone, and it
439 primarily regarded hippocampus, inferior temporal cortex and ventromedial prefrontal cortex.

440 Working memory (WM) abilities also affected the brain responses, especially for the
441 condition NT3, both in older and young individuals. The brain activity after varying the
442 original musical sequence was reduced for participants with lower WM skills.

443 In relation to the behavioural responses, no differences between older and young adults
444 were found when inspecting the accuracy and reaction times associated with the recognition
445 of the previously memorised sequences. Conversely, older adults reported lower accuracy
446 when recognising the varied musical sequences (both NT1 and NT3). No differences were
447 observed for the reaction times.

448 As expected, the results of this study are consistent with our previous research on the brain
449 dynamics underlying the encoding and recognition of musical sequences in healthy young
450 individuals, which showed that the recognition of the previously memorised and varied
451 musical sequence is built over time through a rapid hierarchical pathway of components
452 originated in the auditory cortex and progressing to the hippocampus, ventromedial prefrontal
453 cortex and inferior temporal cortex ²⁵⁻³⁰. Beyond this, the most notable finding of our study is
454 the altered brain functioning observed in older compared to young adults. On the one hand,
455 this occurred through an overall reduction of the brain activity generated in memory brain
456 regions, supporting previous findings which reported diminished brain responses in aging

457 populations in a variety of different contexts, spanning from resting state to automatic neural
458 responses and conscious tasks^{5, 6, 8, 13, 14, 17, 20, 31}. On the other hand, only for the recognition
459 of the previously memorised sequences, older adults showed increased activity in the left
460 auditory cortex. This altered brain functioning supports the hypothesis that neural predictive
461 processes in non-pathological aging are not simply reduced, but qualitatively transformed³².

462 Overall, our results can be very well interpreted within the large framework of the PCT,
463 providing a relevant contribution to the age-related changes of its neural underpinnings. PCT
464 posits that the brain is constantly updating internal models to predict information and stimuli
465 from the external world²². Recently, it has been successfully linked to complex cognitive
466 processes, finding a notable example in the neuroscience of music. Vuust and colleagues^{23, 24}
467 suggested that, while processing music, the brain repeatedly generates hypotheses and
468 predictions about the upcoming unfolding of musical sequences. When the prediction
469 matches the incoming sounds, the brain recognises the music. Conversely, when the
470 expectation is violated by different sounds, predictions errors arise. Our findings point to
471 impaired conscious predictive coding processes in healthy older adults, as evidenced by
472 reduced brain activity during the prediction and recognition of both original and varied
473 musical sequences. As such, they provide novel insights into the brain dynamics of PCT
474 across the lifespan of healthy adults. These results are also coherent with previous studies
475 which showed an age-related reduction of automatic predictive processes such as MMN¹³⁻¹⁵.
476 Notably, our study largely expands on their significance by showing age-related changes of
477 conscious predictive processes and novelty detection and not only automatic responses to
478 subtle environmental irregularities as typically done in MMN studies.

479 Along this line, we revealed decreased activity in older adults during the recognition of the
480 previously memorised musical sequences in brain regions particularly relevant for memory
481 and predictive processes, such as the hippocampus (especially in the right hemisphere)^{33, 34}.
482 Numerous studies have shown the detrimental effects of aging on the hippocampus and
483 memory performance. For instance, it has been shown that aging is associated with reduced
484 hippocampal size^{35, 36} and that it affects the long-term potentiation (LTP) and long-term
485 depression (LTD) occurring in the hippocampal neurons³⁷. The altered size and functionality
486 of LTP and LTD in the hippocampus occurring with aging might be reflected in the reduction
487 of hippocampal activity that we observed in older adults in our study during the recognition
488 of the previously learned musical sequences. The stronger involvement of the hippocampus

489 in the right hemisphere is coherent with the plethora of findings which reported the right-
490 hemispheric dominance in music processing³⁸.

491 Another essential brain region for understanding, predicting and producing language and
492 music is the inferior frontal gyrus^{39, 40}, which also showed a sharp decreased activity in older
493 adults in our study. This is a rather interesting result since there is scarce evidence showing
494 impaired functionality in the inferior frontal gyrus in aging populations, suggesting that this
495 effect may be specifically linked to the age-related changes underlying the prediction and
496 recognition of musical sequences. Moreover, the inferior frontal gyrus does not normally play
497 a pivotal role in the recognition of memorised musical sequences. However, our results
498 suggest that it may provide an additional, relevant contribution to this memory process,
499 which is instead largely attenuated in aging populations, as clearly shown by the contrast
500 between the brain activity of young and older adults. This evidence might also point to a
501 general reduced functionality of the inferior frontal gyrus in older adults, potentially
502 contributing to explain the challenges older adults often face in linguistic, predictive and
503 memory tasks⁴¹⁻⁴³.

504 On a related note, our findings revealed an intriguing pattern of increased activity in the
505 left auditory cortex of older adults during the recognition of musical sequences. This
506 increased activity was observed for the N100 component to the first sound, as well as for the
507 positive component peaking around 350-400 ms after each sound of the sequence. Coherently
508 with PCT, it is plausible that the increased activity in the left auditory cortex is a result of
509 top-down influences from the hippocampus and ventromedial prefrontal and inferior temporal
510 cortices, which are supposed to actively monitor the unfolding musical sequence²⁴. In this
511 case, when they successfully predict the sequence, they require less effort from the left
512 auditory cortex. In a young and more effective brain, the more refined prediction and higher
513 control exerted by those brain regions would result in a reduced activity in the auditory
514 cortex, exactly as we observed in our study.

515 Interestingly, no significant differences were found between older and young adults in
516 terms of accuracy and reaction times when recognising previously memorised sequences.
517 This finding suggests that brain activity may undergo alterations before behavioural
518 manifestations become apparent. This observation raises exciting possibilities for using brain
519 activity as a potential biomarker for the early detection of cognitive decline, which should be
520 further explored by future studies.

521 We also examined the impact of aging on the recognition of varied musical sequences and
522 the prediction error arising when the original sequences were altered. We identified the key
523 involvement of the left and, especially, right hippocampus and bilateral ventromedial
524 prefrontal cortex. The hippocampus is a central brain region for prediction error ^{34, 44} and its
525 reduced activity in older adults suggests that aging is associated with decreased ability to
526 consciously process errors and deviations from previously learned sequences.

527 Similarly, the ventromedial prefrontal cortex, a brain region implicated in reasoning and
528 evaluation processes ⁴⁵, exhibited reduced activity in older adults. In accordance with our
529 findings, studies have shown that age-related changes in the ventromedial prefrontal cortex
530 are associated with decline in cognitive control and decision-making abilities ^{46, 47}. For
531 instance, O'Callaghan and colleagues ⁴⁶ found that individuals with ventromedial prefrontal
532 cortex damage and healthy older adults reported reduced awareness of the presented stimuli
533 during learning tasks. This relates to our results, suggesting that the reduced activity in the
534 ventromedial prefrontal cortex observed in older adults might represent the neural signature
535 of the decreased conscious prediction error and awareness of the musical novelty in aging.

536 To be noted, splitting the older adult participants into two age groups further strengthens
537 the reliability of our previously described results, as it reveals a more pronounced reduction
538 in brain activity in participants older than 68 compared to those aged 60-68. This highlights
539 the progressive nature of age-related changes in brain functioning.

540 Lastly, we showed a relationship between the participants' WM abilities and the brain
541 activity. Participants with higher WM exhibited stronger brain activity, particularly when
542 recognising the varied musical sequences. This finding underscores the potential of using
543 WM as a predictor of preserved brain activity in older adults. In fact, older adults with high
544 WM capacity showed brain activity levels similar to those of young adults with lower WM
545 capacity. This finding is strongly in line with previous research on cognitive reserve,
546 suggesting that higher cognitive abilities in older populations represent a protective factor
547 against mild cognitive impairment and dementia ⁴⁸⁻⁵⁰.

548 In summary, the present study provides valuable novel insights into the impact of aging on
549 the brain function and shows how age is not always related to decline but rather to a
550 comprehensive transformation of brain regions, including the hippocampus, inferior frontal
551 gyrus, and ventromedial prefrontal and auditory cortices. The results provide an important
552 contribution to understanding age-related neural changes and reveal the potential of our

553 methods to identify possible biomarkers for healthy aging and early detection of
554 transformative changes in brain function.
555

556 **Materials and methods**

557

558 **Participants**

559 After removing one participant due to technical issues with the MEG signal, the sample
560 consisted of 76 participants (34 males, 42 females), divided into two age groups: young and
561 older adults. The older adult group consisted of 39 participants (24 females, 15 males) aged
562 60 to 81 years old (mean age: 67.72 ± 5.35 years). The young group included 37 participants
563 (18 females, 19 males) aged 18 to 25 years old (mean age: 21.89 ± 2.05 years). The
564 nationality of all participants was Danish. The inclusion criteria for the participants were the
565 following: (i) normal health (no reported neurological nor psychiatric illness), (ii) age
566 between 18 and 25 years old (young adults' group) and older than 60 years (older adults'
567 group), (iii) normal hearing according to the age group of each participant, (iv) normal sight
568 or corrected to normal sight (e.g., contact lenses), and (v) understanding and acceptance of
569 participant information. The exclusion criteria that we applied were: (i) use of prescribed
570 medication that could affect the central nervous system, (ii) neurological or psychiatric
571 illness, (iii) lack of cooperation or verbal agreement for participating in the study, (iv)
572 magnetic resonance imaging (MRI) contraindications, (v) age between 26 and 59 years old,
573 and impaired hearing (vi).

574 The project was approved by the Institutional Review Board of Aarhus University (case
575 number: DNC-IRB-2021-012). The experimental procedures complied with the Declaration
576 of Helsinki – Ethical Principles for Medical Research. Participants' informed consent was
577 obtained before the beginning of the experiment.

578

579 **Experimental stimuli and design**

580 In this study, we presented participants with an auditory recognition task based on the
581 old/new paradigm that we developed in our previous works ²⁶⁻³⁰. At the same time, we
582 recorded their brain activity using magnetoencephalography (MEG). The participants were
583 required to listen to a brief musical piece (roughly 25 seconds) twice and were instructed to
584 memorise it as best as they could. The musical piece comprised the initial four measures of
585 Johann Sebastian Bach's Prelude No. 2 in C Minor, BWV 847. The wave audio file that we
586 used in the experiment was generated using Finale (MakeMusic, Boulder, CO). The volume
587 of the musical stimuli was set to 60 dB for 67 participants and to 70 dB on average for nine of
588 our participants older than 70 years who presented a very mild hearing impairment, as

589 typically occurring with aging. To limit the adjustment of the volume across participants to
590 only a few of them, we used sounds that almost always fell in the range 125 - 650 Hz, which
591 is only marginally affected by the typical hearing loss occurring with aging⁵¹. Each tone
592 within the piece had the same duration of around 350 ms. In the second phase of the task,
593 participants were presented with 81 musical sequences consisting of five tones and lasting
594 1750 ms. They were then asked to identify whether each sequence was part of the original
595 musical piece (old or memorised sequence [M]) or if it was a different musical sequence
596 (new or novel sequence [N]) (see **Figure 1**). For the purpose of this study, we presented
597 participants with 27 sequences from the original musical piece and created 54 variations of
598 the original melodies. The musical sequences used in the study are depicted in **Figure S1**.
599 The two types of stimuli used in the study were created as follows. The M sequences were
600 comprised of the first five tones from the first three measures of the musical piece. These
601 sequences were presented a total of 27 times, nine times for each sequence. The N sequences
602 were generated by systematically altering the three M sequences (see **Figure 1**). This
603 involved changing every musical tone of the sequence while keeping the first tone (NT1) or
604 the first three tones (NT3) the same as the M sequences. Nine variations were created for
605 each of the original M sequences and each of the two categories of N. As a result, there were
606 27 N sequences for each category and 54 N sequences in total. The variations were created
607 following specific rules:

- 608 • Inverted melodic contour (used twice): this involved creating a variation with a
609 melodic contour that was inverted relative to the original M sequence. (i.e., if the
610 melodic contour of the M sequence was down-down-up-down, the N sequence would
611 be up-up-down-up).
- 612 • Same tone scrambled (used three times): this involved scrambling the remaining tones
613 of the M sequence (e.g., M sequence C-E-D-E-C, was changed into NT1 sequence C-
614 C-E-E-D).
- 615 • Same tone (used three times): this involved using the same tone repeatedly, sometimes
616 varying only the octave (e.g., M sequence C-E-D-E-C, became NT1 sequence C-E⁸-
617 E₈⁻ E₈).
- 618 • Scrambling intervals (used once): this involved scrambling the intervals between the
619 tones (e.g., M sequence 6thm - 2ndm - 2ndm - 3rdm, was changed to NT1 sequence
620 2ndm, 6thm, 3rdm, 2ndm).

621 We adopted this procedure to study the difference between young and older adults with
622 regards to their brain dynamics underlying (i) the recognition of previously memorised
623 auditory sequences and (ii) their conscious detection of the varied sequences.

624

625 **Neural data acquisition**

626 During this study, MEG recordings were conducted at Aarhus University Hospital (AUH),
627 Aarhus, Denmark, using an Elekta Neuromag TRIUX MEG scanner with 306 channels. The
628 data was recorded with an analogue filtering of 0.1 – 330 Hz at a sampling rate of 1000 Hz.
629 To ensure accurate co-registration with the MRI anatomical scans, the head shape of
630 participants and the position of four Head Position Indicator (HPI) coils were registered using
631 a 3D digitizer (Polhemus Fastrak, Colchester, VT, USA). During the MEG recordings, two
632 sets of bipolar electrodes were also used to record cardiac rhythm and eye movements,
633 allowing for removal of electrocardiography (ECG) and electro-oculography (EOG) artifacts
634 in a later stage of the analysis.

635 The MRI scans were recorded on a CE-approved 3T Siemens MRI-scanner at AUH using
636 the following structural T1 sequence parameters: echo time (TE) = 2.61 ms, repetition time
637 (TR) = 2300 ms, reconstructed matrix size = 256 x 256, echo spacing = 7.6 ms, and
638 bandwidth = 290 Hz/Px.

639 The MEG and MRI recordings were conducted on separate days.

640

641 **Working memory, musical expertise and background data**

642 We evaluated domain-general working memory (WM) abilities using the Digit Span and
643 Arithmetic subtests from the Wechsler Adult Intelligence Scale IV's Working Memory index.
644 The Digit Span subtest required participants to listen and repeat sequences of numbers in the
645 same, inverse, or ascending order. The Arithmetic subtest involved solving mathematical
646 operations provided orally by the experimenters without external aids. We combined the raw
647 scores from both subtests to calculate individual WM abilities, with scores ranging from five
648 to 70. Additionally, we assessed formal musical training using the Goldsmiths Musical
649 Sophistication Index (Gold-MSI) questionnaire, which includes 39 questions on musical
650 skills, experience, and habits. We used the Musical Training facet, which estimates an
651 individual's history of formal musical training, and scores range from seven to 49.

652 In addition, we collected general background data such as the years of education. These
653 data were then used as covariates in later stages of the analysis to assess whether they had an

654 impact on the relationship between age and neural data during recognition of auditory
655 sequences.

656

657 **Behavioural data during MEG recording**

658 During the auditory recognition task, we recorded participants' responses and reaction times.
659 We then used this data to estimate differences in response accuracy and average reaction time
660 between young and older participants, and to calculate the impact of sex, years of education,
661 WM abilities, and years of musical training on the behavioural data.

662 We computed two independent multivariate analysis of variance (MANCOVA, Wilk's
663 Lambda [Λ], $\alpha = .05$)⁵² using group as the independent variable (young vs older) and years
664 of education, WM scores, years of musical training, and sex as covariates. In one
665 MANCOVA, number of correct responses (divided into M, NT1 and NT3) were used as the
666 three dependent variables. In the other MANCOVA, average reaction time during correct
667 responses (divided into M, NT1, and NT3) were used as the three dependent variables. The
668 effect size was calculated using partial eta squared (i.e., partial η^2).

669 To determine the effects of the independent variable and covariate, univariate analyses of
670 covariance (ANCOVA) were computed individually for each of the dependent variables and
671 statistically significant covariates.

672

673 **MEG data pre-processing**

674 The MEG data obtained from 204 planar gradiometers and 102 magnetometers was initially
675 subjected to pre-processing with MaxFilter⁵³, which helped to reduce external interferences.
676 We applied signal space separation and the following MaxFilter parameters: spatiotemporal
677 signal space separation [SSS], down-sample from 1000Hz to 250Hz, correlation limit
678 between inner and outer subspaces used to reject overlapping intersecting inner/outer signals
679 during spatiotemporal SSS: 0.98, movement compensation using cHPI coils (default step
680 size: 10 ms).

681 After conversion to Statistical Parametric Mapping (SPM) format, the data was pre-
682 processed and analysed in MATLAB using both in-house-built codes (LBPD,
683 <https://github.com/leonardob92/LBPD-1.0.git>) and the freely available Oxford Centre for
684 Human Brain Activity (OHBA) Software Library (OSL)⁵⁴ (<https://ohba-analysis.github.io/osl-docs/>), which utilises Fieldtrip⁵⁵, FSL⁵⁶, and SPM⁵⁷ toolboxes. We
686 visually inspected the filtered MEG data using OSLview to remove large artifacts, which

687 accounted for less than 0.1% of the total data. We employed independent component analysis
688 (ICA) to separate and remove eyeblink and heartbeat interference from the brain data ⁵⁸. This
689 involved decomposing the original signal into independent components, discarding the
690 components that detected eyeblink and heartbeat activities, and reconstructing the signal
691 using the remaining components. We then epoched the signal into 81 trials and baseline-
692 corrected it by subtracting the mean signal recorded in the baseline from the post-stimulus
693 brain signal. The trials lasted 3500 ms (3400 ms after the onset of the first tone of the musical
694 sequence plus 100 ms of baseline time) and were categorised into three groups (M, NT1,
695 NT3) with 27 trials each.

696

697 **MEG sensor level and aging**

698 To assess the difference between the brain activity of young and older adults while they
699 recognised the musical sequences, we calculated several independent samples t-tests with
700 unequal variances and then corrected for multiple comparisons using cluster-based Monte-
701 Carlo simulations (MCS). As it is common in MEG and EEG task studies ^{59, 60}, we computed
702 the average over trials in each condition before performing t-tests, which resulted in three
703 mean trials (M, NT1, NT3). For each condition separately, we computed a t-test for each
704 MEG magnetometer channel and each time-point between 0 and 2000 ms, contrasting the
705 brain activity of young and older adults. We then reshaped the matrix to obtain a two-
706 dimensional (2D) approximation of the MEG channels layout for each time-point, binarising
707 it based on the *p*-values obtained from the previous t-tests (threshold = .05) and the sign of t-
708 values. The resulting 3D matrix (*MX*, 2D x time) consisted of 0s when the t-test was not
709 significant and 1s when it was. To correct for multiple comparisons, we identified clusters of
710 1s and assessed their significance using MCS. Specifically, we performed 1000 permutations
711 of the elements of the original binary matrix *MX*, identified the maximum cluster size of 1s,
712 and built the distribution of the 1000 maximum cluster sizes. We considered clusters that had
713 a size bigger than the 99.9% maximum cluster sizes of the permuted data to be significant.
714 We applied the MCS procedure to the absolute values of magnetometer MEG channels for
715 both young versus older adults and vice versa.

716

717 **Source reconstruction**

718 MEG provides excellent temporal resolution, but to fully understand the brain activity
719 underlying complex cognitive tasks, the spatial component of the brain activity must also be

720 identified. To estimate the sources of the brain that generated the signal recorded by the MEG
721 sensors, we computed a source reconstruction protocol using a combination of in-house-built
722 codes and codes available in OSL, SPM, and FieldTrip.

723 The source reconstruction analysis consists of designing a forward model and computing
724 the inverse solution. The forward model considers each brain source as an active dipole and
725 describes how the unitary strength of each dipole is reflected over all MEG sensors. We used
726 magnetometer channels and an 8-mm grid to obtain 3559 dipole locations within the whole
727 brain (voxels). After co-registering the individual structural T1 data with the fiducial points
728 (i.e., information about head landmarks such as the nasion and the left and right pre-auricular
729 points), we computed the forward model using the widely used “Single Shell” method, which
730 resulted in a leadfield model stored in matrix L (sources x MEG channels)⁶¹. In cases where
731 structural T1 was unavailable, we used a template (MNI152-T1 with 8-mm spatial resolution)
732 for the leadfield computation.

733 Afterwards, we calculated the inverse solution, using the established beamforming
734 method, which is a popular and effective algorithm available in the field of neuroscience. The
735 process involves utilising a distinct series of weights that are applied successively to the
736 source positions, enabling the separation of the impact of each source on the activity detected
737 by the MEG channels. This is carried out for every instance of the brain data captured. The
738 beamforming inverse solution is comprised of several key stages, which can be outlined as
739 follows.

740 The data measured by the MEG sensors (B) at time t , can be described by the following
741 equation (1):

742

$$B_{(t)} = L * Q_{(n_i,t)} + \quad (1)$$

743

744 where L is the leadfield model, Q is the dipole matrix which carries the activity of each active
745 dipole (q) over time, and \square is noise (see Huang and colleagues for details⁶²). In order to
746 resolve the inverse problem, Q has to be computed. In the beamforming algorithm, to
747 calculate Q , a series of weights have to be computed and applied to the MEG sensors at each
748 timepoint. This is done for each single dipole q and shown in equation (2):

749

$$q_{(t)} = W^T * B_{(t)} \quad (2)$$

750

751 To obtain q , the weights W have to be computed (here, the subscript T indicates the transpose
752 matrix). The beamforming method relies on the matrix multiplication between L and the
753 covariance matrix between MEG sensors (C). This matrix is calculated on the concatenated
754 experimental trials. More specifically, for each brain source n , the weights W_n are calculated
755 as shown in equation (3):

756

$$W_{(n)} = (L_{(n)}^T * C^{-1} * L_{(n)})^{-1} * L_{(n)}^T * C^{-1} \quad (3)$$

757

758 The calculation of the leadfield model was performed for the three main orientations of each
759 brain source (dipole), as done in the field (see, for example, Nolte ⁶¹). Then, prior to
760 computing the weights, the orientations were reduced (from three to one) by using the
761 singular value decomposition algorithm on the matrix multiplication reported in equation (4).
762 This procedure is widely adopted and used to simplify the beamforming output ^{63, 64}.

763

$$L = svd(l^T * C^{-1} * l)^{-1} \quad (4)$$

764

765 In this context, l denotes the leadfield model with the three orientations, while L is the
766 resolved one-orientation model that was used in the estimation of the brain sources in
767 equation (3). The weights were then applied to each brain source and timepoint, with the
768 covariance matrix C being computed based on the continuous signal that resulted from
769 concatenating the trials across all experimental conditions. To counterbalance the source
770 reconstruction bias towards the head's centre, the weights were normalised according to
771 Luckhoo and colleagues ⁶⁴. Since we worked on evoked responses, the weights were applied
772 to the neural activity averaged over trials.

773 This procedure allowed us to obtain a time series for each of the 3559 brain sources and
774 each experimental condition. To adjust the sign ambiguity of the evoked responses time
775 series for each brain source, the sign was matched with the N100 response to the first tone of
776 the auditory sequences ²⁶⁻³⁰.

777

778 **MEG source level and aging**

779 For each of the significant clusters emerged from the previous analysis at the MEG sensor
780 level, we contrasted the brain activity of young versus older adults. We averaged the time
781 series of all brain sources over the time-window of each significant cluster and computed

782 independent-sample t-tests contrasting the brain activity of young versus older adults. This
783 procedure was computed independently for the three experimental conditions (M, NT1,
784 NT3). Finally, we corrected for multiple comparisons using a 3D cluster-based MCS ($\alpha =$
785 .005 [older vs young adults], $\alpha = .05$ [young vs older adults], p -value = .001). Here, we used
786 a stricter α level for older vs young adults since the difference in their brain activity was
787 particularly strong and we wanted to highlight the main focus of such differences. For this
788 procedure, we first determined the sizes of significant clusters consisting of neighbouring
789 brain voxels. Subsequently, we generated 1000 permutations of the initial data and estimated
790 the sizes of significant clusters formed by neighbouring brain voxels in each permutation.
791 This process yielded a reference distribution of the largest cluster sizes observed in the
792 permuted data. Finally, we identified original clusters as significant if their size was larger
793 than 99.99% of the clusters in the reference distribution. Further details on the MCS
794 algorithm can be found in previous works by Bonetti and colleagues ²⁶⁻³⁰.

795

796 **Functional regions of interests (ROIs)**

797 We computed a complementary analysis by investigating the difference between the brain
798 activity of young versus older adults in a selected array of functional ROIs, previously
799 described by Bonetti, Fernández Rubio, Carlomagno, Pantazis, Vuust and Kringelbach ²⁸.
800 These were derived from the whole-brain analysis of the active brain regions of young adults
801 during recognition of the same musical sequences used in the current study. These areas
802 roughly corresponded to the bilateral medial cingulate gyrus (MC), bilateral ventromedial
803 prefrontal cortex (VMPFC), left (HITL) and right hippocampal area and inferior temporal
804 cortex (HITR), and left (ACL) and right auditory cortex (ACR). In addition, we incorporated
805 the left (IFGL) and right inferior frontal gyrus (IFGR) because these regions displayed
806 marked differences between young and older adults.

807 This additional analysis allowed us to reconstruct with greater precision the time series of
808 each brain region that played a central role in auditory sequence recognition. Thus, while it
809 did not provide additional information to the previous analysis, it refined its significance. In
810 **Table S4**, we reported the Montreal Neurological Institute (MNI) coordinates of each voxel
811 forming the eight ROIs. The ROIs are visually displayed in **Figure S2**.

812

813 **Aging and ROIs time series**

814 We contrasted the brain activity of young versus older adults by computing an independent-
815 sample t-test for each ROI, timepoint, and condition. We corrected for multiple comparisons
816 using 1D cluster-based MCS ($\alpha = .05$, MCS p -value = .001). First, we identified the clusters
817 of the significant values which were continuous in time. Second, we performed 1000
818 permutations, consisting of randomising the significant values obtained from the t-tests. For
819 each permutation, we then extracted the maximum cluster size, and we built their reference
820 distribution. To summarise, we considered significant the original clusters that were larger
821 than the 99.99% of the clusters emerged in the permutations. Additional details on this
822 procedure can be found in previous works by Bonetti and colleagues ²⁶⁻³⁰.

823

824 **WM, musical expertise, education level, aging and neural data**

825 We computed two additional analyses to assess whether potential confounding variables had
826 an impact on the relationship between aging and the neural responses underlying the
827 recognition of the musical sequences.

828 In the first analysis we computed three independent multivariate analyses of covariance
829 (MANCOVAs), one for each experimental condition (Wilks Lambda [Λ], $\alpha = .05$). In each
830 MANCOVA the dependent variables were the neural data for the eight ROIs, the independent
831 variable was age, and the covariates were years of formal musical expertise, sex, WM, and
832 years of formal education that participants received. To be noted, the neural data was
833 collapsed into one single value for each ROI and participant. This was computed by
834 averaging the main response (neural peak ± 20 ms) to each tone in the M condition. With
835 regards to the N conditions, we selected the main response (neural peak ± 20 ms) to the tone
836 that introduced the variation in the sequence. This analysis was conducted in R ⁶⁵.

837 The second analysis consisted of computing analyses of variance (ANOVAs) for each
838 time-point and each ROI and then using the same cluster-based 1D MCS to correct for
839 multiple comparisons that we described in the previous paragraphs.

840 In this case, we computed two independent sets of ANOVAs. In the first one, we used
841 one-way ANOVAs contrasting three age-groups: young (younger than 25), older adults 60-68
842 (age between 60 and 68), and older adults > 68 (older than 68). In the second set, we used
843 two-way ANOVAs with the following levels: WM (high and low performers) and age (young
844 and older adults). This allowed us to further test the changes in the brain activity over
845 different age-groups as well as to better highlight the impact of WM on the ROIs time series.

846 **Figures 5** and **6** report the ROIs which showed the strongest results, while **Tables S6** and
847 **S7** disclosed the complete details of the statistical results.

848 To be noted, four participants (three young and one older adult) did not complete the WM
849 assessment. For this reason, the analyses described in this paragraph were computed with a
850 sample of 72 participants.

851
852

853 ***Data availability***

854 The codes are available at the following links:

855 https://github.com/leonardob92/MEG_Aging_Bach.git

856 <https://github.com/leonardob92/LBPD-1.0.git>

857 The multimodal neuroimaging data related to the experiment is available upon reasonable
858 request.

859

860

861 ***Acknowledgements***

862 The Center for Music in the Brain (MIB) is funded by the Danish National Research
863 Foundation (project number DNRF117).

864 LB is supported by Carlsberg Foundation (CF20-0239), Lundbeck Foundation (Talent
865 Prize 2022), Center for Music in the Brain, Linacre College of the University of Oxford
866 (Lucy Halsall fund), Society for Education and Music Psychology (SEMPRE's 50th
867 Anniversary Awards Scheme), and Nordic Mensa Fund.

868 MLK is supported by Center for Music in the Brain and Centre for Eudaimonia and
869 Human Flourishing, which is funded by the Pettit and Carlsberg Foundations.

870

871 ***Author contributions***

872 LB, GFR, EB and MLK conceived the hypotheses. LB, GFR and ERO designed the study.
873 LB, MLK, EB and PV recruited the resources for the experiment. LB, GFR, ERO and FC
874 collected the data. LB, GFR and performed pre-processing and statistical analysis. MLK, EB,
875 ML, SAK, AC and PV provided essential help to interpret and frame the results within the
876 neuroscientific literature. GFR and LB wrote the first draft of the manuscript. LB, GFR and
877 MLK prepared the figures. All the authors contributed to and approved the final version of
878 the manuscript.

879

880

881 ***Competing interests' statement***

882 The authors declare no competing interests.

883

884 ***SUPPLEMENTARY MATERIAL***

885

886 Supplementary materials related to this study and organised as supplementary figures (*i*) and
887 tables (*ii*). In the cases when the supplementary tables were too large to be reported in the
888 current document, they have been exported to Excel files that can be found at the following
889 link:

890 <https://drive.google.com/drive/folders/1mCDD1Eghm5W7aJ9jtjl-9NczNB457ROQ?usp=sharing>

892

893

894 **SUPPLEMENTARY FIGURES**

895

896

The image displays a musical score with multiple staves of music. The first staff is labeled 'Melody 1' and shows a sequence of notes with labels below: m1, m1t1e1, m1t3e1. The second staff is labeled 'Inverted Melodic Contour I' and shows a sequence of notes with labels below: m1t1e2, m1t3e2, m1t1e3, m1t3e3. The third staff is labeled 'Same Tone Scrambled I' and shows a sequence of notes with labels below: m1t1e4, m1t3e4, m1t1e5, m1t3e5. The fourth staff is labeled 'Same Tone II' and shows a sequence of notes with labels below: m1t1e6, m1t3e6, m1t1e7, m1t3e7. The fifth staff is labeled 'Scrambling Intervals' and shows a sequence of notes with labels below: m1t1e8, m1t3e8, m1t1e9, m1t3e9. The sixth staff is labeled 'Inverted Melodic Contour II' and shows a sequence of notes with labels below: m1t1e1, m2t1e1, m2t3e1. The seventh staff is labeled 'Same Tone Scrambled III' and shows a sequence of notes with labels below: m2t1e2, m2t3e2, m2t1e3, m2t3e3. The eighth staff is labeled 'Same Tone III' and shows a sequence of notes with labels below: m2t1e4, m2t3e4, m2t1e5, m2t3e5. The ninth staff is labeled 'Melody 2' and shows a sequence of notes with labels below: m2, m2t1e1, m2t3e1. The tenth staff is labeled 'Inverted Melodic Contour I' and shows a sequence of notes with labels below: m2t1e2, m2t3e2, m2t1e3, m2t3e3.

897

898

899

900

901

902

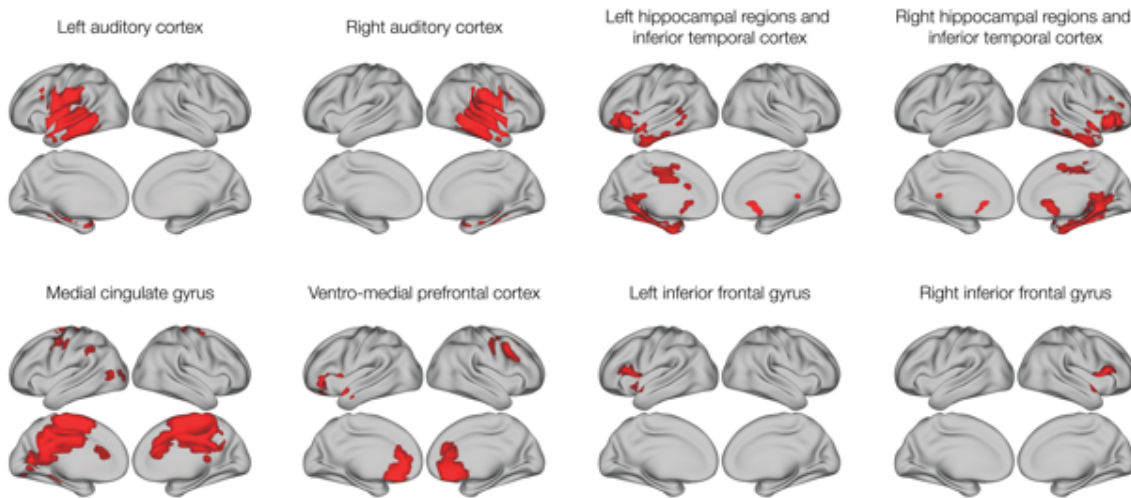
903 **Figure S1. Temporal sequences used in the experiment.**

904 The figure shows all temporal sequences used in the experiment, providing detailed information on how they
905 were created. The M sequences were three and comprised the first five tones of the first three measures of the
906 musical piece. These three sequences were presented nine times each, for a total of 27 trials. The N sequences
907 were created through systematic variations of the three M sequences. This procedure consisted of changing
908 every musical tone of the sequence after the first (NT1) or third (NT3) tone. We created nine variations for each
909 of the original M sequences and each of the four categories of N. This resulted in 27 N sequences for each
910 category, and 54 N in total. To be noted, as shown in this figure, the variations were created according to the
911 following rules: (i) Inverted melodic contours (used twice): the melodic contour of the variation was inverted
912 with respect to the original M sequence (i.e., if the M sequence had the following melodic contour: down-down-
913 up-down, the N sequence would be: up-up-down-up); (ii) Same tone scrambled (used three times): the
914 remaining tones of the M sequence were scrambled (e.g., M sequence: C-E-D-E-C, was converted into NT1
915 sequence: C-C-E-E-D); (iii) Same tone (used three times): the same tone was repeatedly used, in some cases
916 varying only the octave (e.g., M sequence: C-E-D-E-C, was transformed into NT1 sequence: C-E⁸ E⁸ E₈ E₈);
917 (iv) Scrambling intervals (used once): the intervals between the tones were scrambled (e.g., M sequence: 6thm -
918 2ndm - 2ndm - 3rdm, was adapted to NT1 sequence: 2ndm, 6thm, 3rdm, 2ndm).

919

920

Regions of interest



921

922

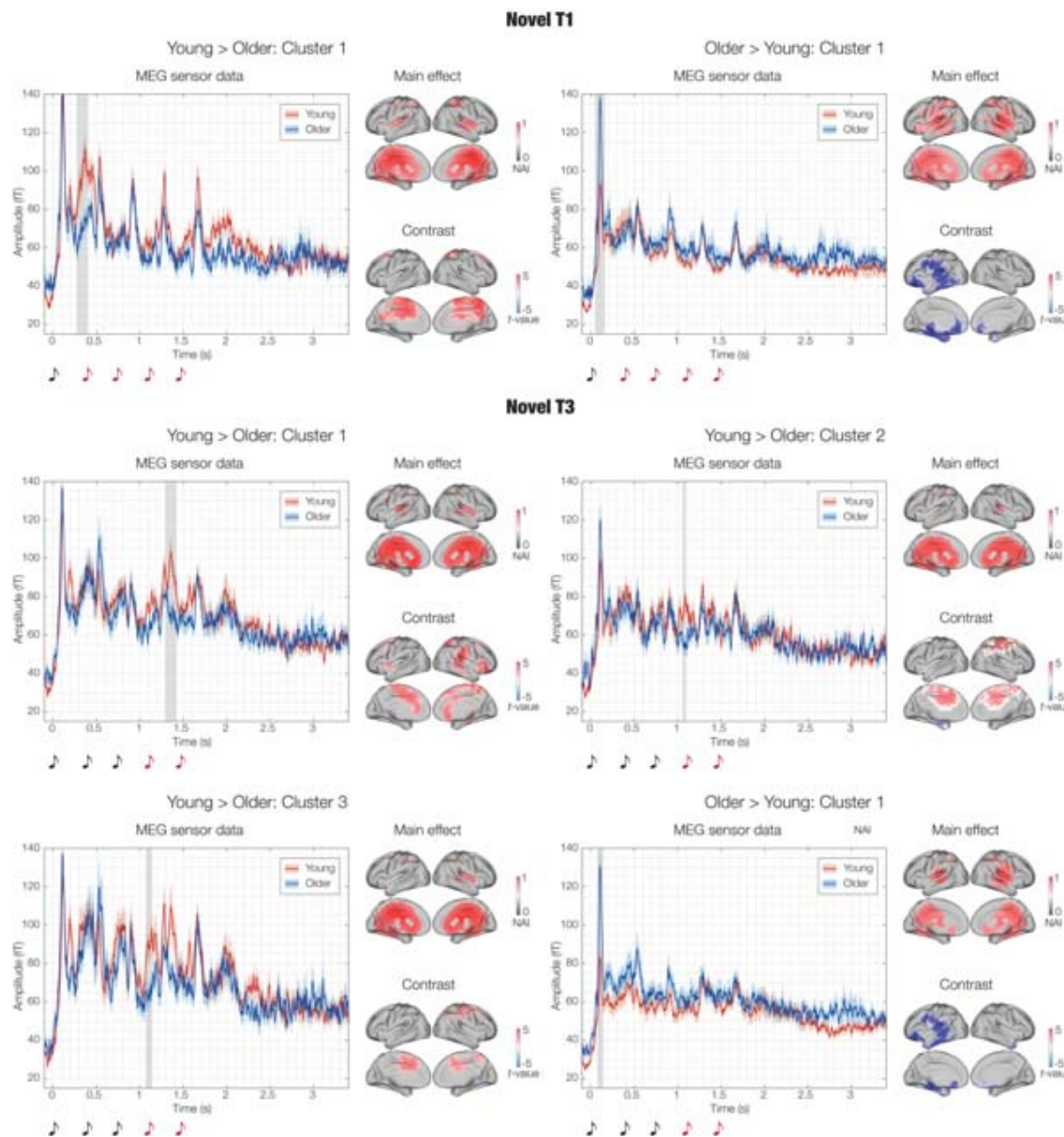
923 **Figure S2. Brain parcellation.**

924 *The eight ROIs used in the study: left (i) and right auditory cortex (ii); left (iii) and right hippocampal regions*
925 *and inferior temporal cortex (iv); medial cingulate gyrus (v), ventromedial prefrontal cortex (vi); left (vii) and*
926 *right inferior frontal gyrus (viii).*

927

928

929



930

931

932 *Figure S3. Impact of aging on the brain activity underlying the recognition of previously memorised musical*
 933 *sequences.*

934 *Significant contrasts between the brain activity of young and older adults during the recognition of previously*
 935 *memorised musical sequences. For each significant cluster, the left plot shows the amplitude of the brain signal*
 936 *recorded for young (red) and older adults (blue). Shaded red and blue areas depict standard errors, while grey*
 937 *areas refer to the significant time-window for the cluster. The plot refers to the average over the absolute values*
 938 *of the magnetometer channels forming the significant clusters outputted by the MEG sensors MCS. The plot on*
 939 *the right shows the neural sources in the time-window of the significant MEG sensors cluster. The top plot*
 940 *shows the main effect over all participants (the colorbar indicates the reconstructed brain activity standardised*

941 *between 0 and 1), while the bottom plot shows the contrast between the brain activity of young versus older*
942 *adults (the colorbar indicates the t-value of the contrast). The first five clusters refer to the contrasts where the*
943 *brain activity was stronger for young versus older adults. The last cluster refers to the contrasts where the brain*
944 *activity was stronger for older versus young adults. **Table 2** reports the key statistics of these analyses, while*
945 ***Table S1** shows the complete results.*

946

947

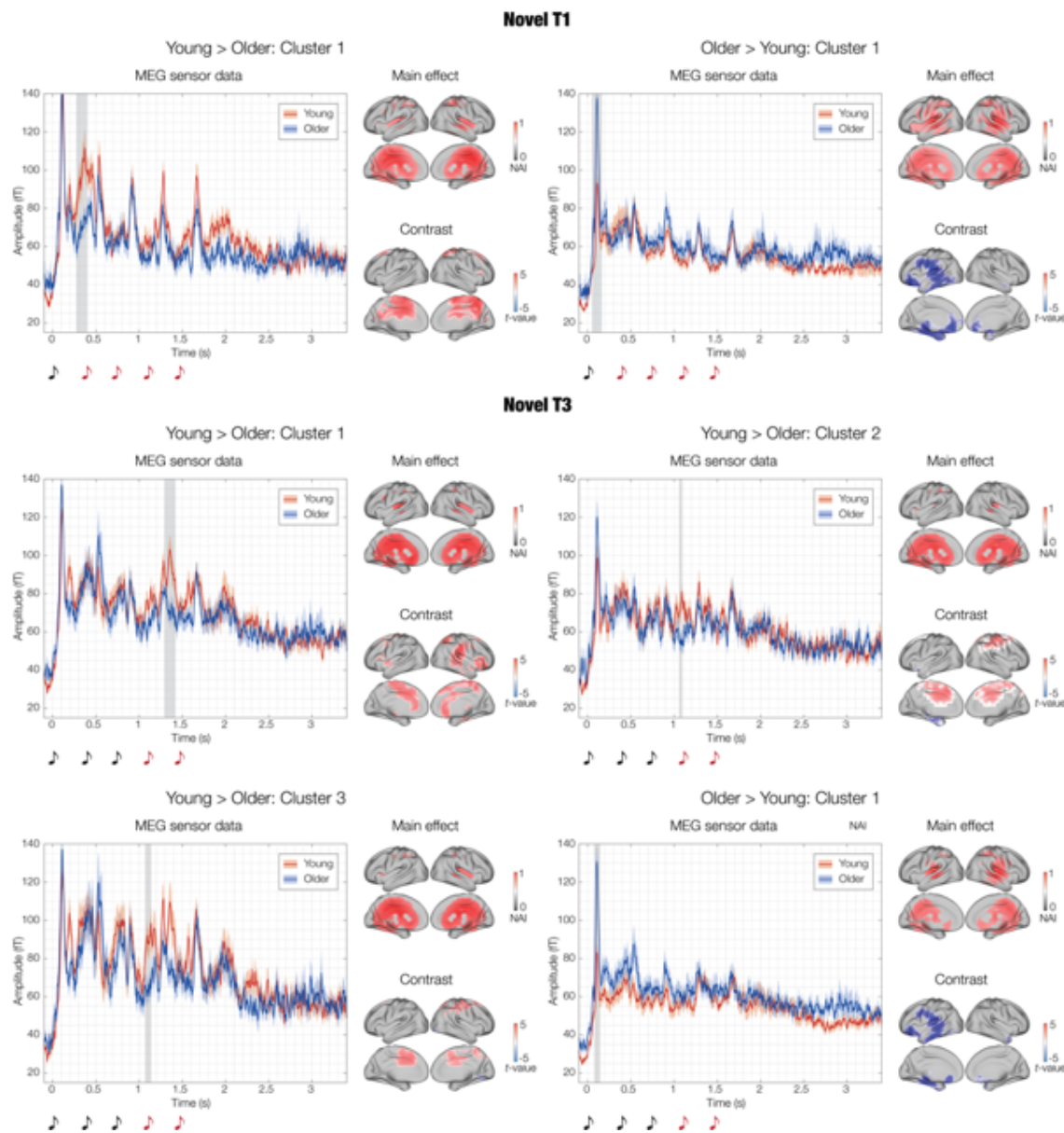


Figure S4. Impact of aging on the brain activity underlying the recognition of the varied (novel) musical sequences.

Significant contrasts between the brain activity of young and older adults during the recognition of the varied musical sequences (NT1 and NT3). For each significant cluster, the left plot shows the amplitude of the brain signal recorded for young (red) and older adults (blue). Shaded red and blue areas depict standard errors, while grey areas refer to the significant time-window for the cluster. The plot refers to the average over the absolute values of the magnetometer channels forming the significant clusters outputted by the MEG sensors MCS. The plot on the right shows the neural sources in the time-window of the significant MEG sensors cluster. The top plot shows the main effect over all participants (the colorbar indicates the reconstructed brain activity

959 standardised between 0 and 1), while the bottom plot shows the contrast between the brain activity of young
960 versus older adults (the colorbar indicates the *t*-value of the contrast). The first two clusters refer to NT1 (on the
961 left the contrasts where the brain activity was stronger for young versus older adults and on the right vice
962 versa). The last four clusters refer to NT3 (the first three clusters relate to the contrasts where the brain activity
963 was stronger for older versus young adults, while the last one vice versa). **Table 2** reports the key statistics of
964 these analyses, while **Table S1** shows the complete results.

965

966

967 **SUPPLEMENTARY TABLES**

968

969 **Table S1. Detailed information on significant clusters for MEG sensor data**

970 *Significant clusters of MEG sensors emerged from MCS contrasting the brain activity of young versus older*
971 *adults, independently for the three experimental conditions (M, NT1, NT3). The table illustrates the clusters*
972 *with regards to significant channels, sizes, maximum t-values and time-windows.*

973

974 **Table S2. Source reconstruction main effect.**

975 *Main effect for the source reconstruction performed in the time-windows of the significant clusters at MEG*
976 *sensor level. Results are reported independently for each cluster and contrast, and comprise the brain region,*
977 *brain hemisphere, standardised neural index and MNI coordinates for each voxel.*

978

979 **Table S3. Young versus older adults in MEG source space.**

980 *Significant MEG source clusters of differential brain activity between young and older adults performed in the*
981 *time-windows of the significant clusters at MEG sensor level. Results are reported independently for each*
982 *cluster and contrast, and comprise the brain region, brain hemisphere, t-value and MNI coordinates for each*
983 *voxel.*

984

985 **Table S4. ROIs coordinates.**

986 *MNI coordinates for each of the voxels forming the eight ROIs.*

987

988 **Table S5. ROIs time series.**

989 *Significant clusters of differential brain activity between young and older adults for the eight ROIs used in the*
990 *study. Results are reported independently for the eight ROIs and for each experimental condition (M, NT1,*
991 *NT3), and comprise cluster size, p-value, temporal extent of the clusters and peak t-value within the cluster.*

992

993 **Table S6. ROIs time series and WM.**

994 *Significant clusters of differential brain activity observed by contrasting the following four categories of*
995 *participants: young adults with high WM (i), young adults with low WM (ii), older adults with high WM (iii) and*
996 *older adults with low WM (iv). Results are reported independently for the eight ROIs and for each experimental*
997 *condition (M, NT1, NT3), and comprise cluster size, p-value, temporal extent of the clusters and peak F-value*
998 *within the cluster.*

999

1000 **Table S7. ROIs time series and three age groups.**

1001 *Significant clusters of differential brain activity observed by contrasting the following three categories of*
1002 *participants: young adults (i), older adults aged between 60 and 68 years old (ii) and older adults older than 68*
1003 *years old (iii). Results are reported independently for the eight ROIs and for each experimental condition (M,*

1004 *NT1, NT3), and comprise cluster size, p-value, temporal extent of the clusters and peak F-value within the*
1005 *cluster.*

1006 **References**

- 1007 1. Lenox-Smith, A., Reed, C., Lebrec, J., Belger, M. & Jones, R.W. Potential cost savings to
1008 be made by slowing cognitive decline in mild Alzheimer's disease dementia using a model
1009 derived from the UK GERA observational study. *BMC geriatrics* **18**, 1-6 (2018).
- 1010 2. Parra, M.A., Butler, S., McGeown, W.J., Nicholls, L.A.B. & Robertson, D.J. Globalising
1011 strategies to meet global challenges: the case of ageing and dementia. *Journal of global*
1012 *health* **9** (2019).
- 1013 3. Bishop, N.A., Lu, T. & Yankner, B.A. Neural mechanisms of ageing and cognitive
1014 decline. *Nature* **464**, 529-535 (2010).
- 1015 4. Kumar, A., Singh, A. & Ekaivali. A review on Alzheimer's disease pathophysiology and its
1016 management: an update. *Pharmacol Rep* **67**, 195-203 (2015).
- 1017 5. Tibon, R., *et al.* Transient neural network dynamics in cognitive ageing. *Neurobiol Aging*
1018 **105**, 217-228 (2021).
- 1019 6. Mary, A., *et al.* Age-related differences in practice-dependent resting-state functional
1020 connectivity related to motor sequence learning. *Hum Brain Mapp* **38**, 923-937 (2017).
- 1021 7. Alu, F., *et al.* Entropy modulation of electroencephalographic signals in physiological
1022 aging. *Mech Ageing Dev* **196**, 111472 (2021).
- 1023 8. Babiloni, C., *et al.* Sources of cortical rhythms in adults during physiological aging: a
1024 multicentric EEG study. *Hum Brain Mapp* **27**, 162-172 (2006).
- 1025 9. Naatanen, R. & Picton, T. The N1 wave of the human electric and magnetic response to
1026 sound: a review and an analysis of the component structure. *Psychophysiology* **24**, 375-425
1027 (1987).
- 1028 10. Bonetti, L., *et al.* Auditory sensory memory and working memory skills: association
1029 between frontal MMN and performance scores. *Brain research* **1700**, 86-98 (2018).
- 1030 11. Bonetti, L., Haumann, N., Vuust, P., Kliuchko, M. & Brattico, E. Risk of depression
1031 enhances auditory Pitch discrimination in the brain as indexed by the mismatch negativity.
1032 *Clinical Neurophysiology* **128**, 1923-1936 (2017).
- 1033 12. Bonetti, L., *et al.* Whole-brain computation of cognitive versus acoustic errors in
1034 music: A mismatch negativity study. *Neuroimage: Reports* **2**, 100145 (2022).
- 1035 13. Cheng, C.H., Baillet, S., Hsiao, F.J. & Lin, Y.Y. Effects of aging on neuromagnetic
1036 mismatch responses to pitch changes. *Neurosci Lett* **544**, 20-24 (2013).

1037 14. Cheng, C.H., Wang, P.N., Hsu, W.Y. & Lin, Y.Y. Inadequate inhibition of redundant
1038 auditory inputs in Alzheimer's disease: an MEG study. *Biol Psychol* **89**, 365-373 (2012).

1039 15. Kisley, M.A., Davalos, D.B., Engleman, L.L., Guinther, P.M. & Davis, H.P. Age-
1040 related change in neural processing of time-dependent stimulus features. *Brain Res Cogn*
1041 *Brain Res* **25**, 913-925 (2005).

1042 16. Sardone, R., *et al.* The Age-Related Central Auditory Processing Disorder: Silent
1043 Impairment of the Cognitive Ear. *Front Neurosci* **13**, 619 (2019).

1044 17. Gajewski, P.D. & Falkenstein, M. Age-related effects on ERP and oscillatory EEG-
1045 dynamics in a 2-back task. *Journal of Psychophysiology* (2014).

1046 18. Vaden, R.J., Hutcheson, N.L., McCollum, L.A., Kentros, J. & Visscher, K.M. Older
1047 adults, unlike younger adults, do not modulate alpha power to suppress irrelevant
1048 information. *NeuroImage* **63**, 1127-1133 (2012).

1049 19. Federmeier, K.D., McLennan, D.B., De Ochoa, E. & Kutas, M. The impact of
1050 semantic memory organization and sentence context information on spoken language
1051 processing by younger and older adults: an ERP study. *Psychophysiology* **39**, 133-146
1052 (2002).

1053 20. Babiloni, C., *et al.* Human alpha rhythms during visual delayed choice reaction time
1054 tasks: a magnetoencephalography study. *Hum Brain Mapp* **24**, 184-192 (2005).

1055 21. Costa, M., Vuust, P., Kringelbach, M.L. & Bonetti, L. Age-related brain mechanisms
1056 underlying short-term recognition of musical sequences: An EEG study. *bioRxiv*, 2023.2003.
1057 2012.532256 (2023).

1058 22. Friston, K. Predictive coding, precision and synchrony. *Cognitive neuroscience* **3**,
1059 238-239 (2012).

1060 23. Koelsch, S., Vuust, P. & Friston, K. Predictive processes and the peculiar case of
1061 music. *Trends in cognitive sciences* **23**, 63-77 (2019).

1062 24. Vuust, P., Heggli, O.A., Friston, K.J. & Kringelbach, M.L. Music in the brain. *Nature*
1063 *Reviews Neuroscience* **23**, 287-305 (2022).

1064 25. Bonetti, L., *et al.* Rapid encoding of musical tones discovered in whole-brain
1065 connectivity. *NeuroImage* **245**, 118735 (2021).

1066 26. Bonetti, L., *et al.* Brain recognition of previously learned versus novel temporal
1067 sequences: a differential simultaneous processing. *Cerebral Cortex*, bhac439 (2022).

1068 27. Bonetti, L., *et al.* Spatiotemporal brain dynamics during recognition of the music of
1069 Johann Sebastian Bach. *Biorxiv* (2020).

1070 28. Bonetti, L., *et al.* Revealing the spacetime hierarchical whole-brain dynamics of
1071 auditory predictive coding. *bioRxiv* (2022).

1072 29. Fernandez-Rubio, G., *et al.* Magnetoencephalography recordings reveal the
1073 spatiotemporal dynamics of recognition memory for complex versus simple auditory
1074 sequences. *Commun Biol* **5**, 1272 (2022).

1075 30. Fernández-Rubio, G., Carlomagno, F., Vuust, P., Kringelbach, M.L. & Bonetti, L.
1076 Associations between abstract working memory abilities and brain activity underlying long-
1077 term recognition of auditory sequences. *PNAS Nexus* **1**, pgac216 (2022).

1078 31. Guran, C.A., Herweg, N.A. & Bunzeck, N. Age-Related Decreases in the Retrieval
1079 Practice Effect Directly Relate to Changes in Alpha-Beta Oscillations. *J Neurosci* **39**, 4344-
1080 4352 (2019).

1081 32. Brown, R.M., Gruijters, S.L.K. & Kotz, S.A. Prediction in the Aging Brain: Merging
1082 Cognitive, Neurological, and Evolutionary Perspectives. *J Gerontol B Psychol Sci Soc Sci* **77**,
1083 1580-1591 (2022).

1084 33. Hasselmo, M.E. A Handbook for Modeling Hippocampal Circuits. (Frontiers
1085 Research Foundation, 2011).

1086 34. Barron, H.C., Auksztulewicz, R. & Friston, K. Prediction and memory: A predictive
1087 coding account. *Prog Neurobiol* **192**, 101821 (2020).

1088 35. Fotuhi, M., Do, D. & Jack, C. Modifiable factors that alter the size of the
1089 hippocampus with ageing. *Nature Reviews Neurology* **8**, 189-202 (2012).

1090 36. Grady, C. The cognitive neuroscience of ageing. *Nat Rev Neurosci* **13**, 491-505
1091 (2012).

1092 37. Boric, K., Munoz, P., Gallagher, M. & Kirkwood, A. Potential adaptive function for
1093 altered long-term potentiation mechanisms in aging hippocampus. *J Neurosci* **28**, 8034-8039
1094 (2008).

1095 38. Albouy, P., Benjamin, L., Morillon, B. & Zatorre, R.J. Distinct sensitivity to
1096 spectrotemporal modulation supports brain asymmetry for speech and melody. *Science* **367**,
1097 1043-1047 (2020).

1098 39. Maess, B., Koelsch, S., Gunter, T.C. & Friederici, A.D. Musical syntax is processed
1099 in Broca's area: an MEG study. *Nature neuroscience* **4**, 540-545 (2001).

1100 40. Vuust, P., Roepstorff, A., Wallentin, M., Mouridsen, K. & Ostergaard, L. It don't
1101 mean a thing... Keeping the rhythm during polyrhythmic tension, activates language areas
1102 (BA47). *Neuroimage* **31**, 832-841 (2006).

1103 41. Rubio, G.F., *et al.* Age and musical training effects on auditory short-term, long-term,
1104 and working memory. *bioRxiv*, 2022.2008. 2031.506048 (2022).

1105 42. Juan, S.M. & Adlard, P.A. Ageing and cognition. *Biochemistry and cell biology of*
1106 *ageing: part II clinical science*, 107-122 (2019).

1107 43. Gillis, M., Kries, J., Vandermosten, M. & Francart, T. Neural tracking of linguistic
1108 and acoustic speech representations decreases with advancing age. *Neuroimage* **267**, 119841
1109 (2023).

1110 44. Stachenfeld, K.L., Botvinick, M.M. & Gershman, S.J. The hippocampus as a
1111 predictive map. *Nature neuroscience* **20**, 1643-1653 (2017).

1112 45. Christakou, A., Brammer, M., Giampietro, V. & Rubia, K. Right ventromedial and
1113 dorsolateral prefrontal cortices mediate adaptive decisions under ambiguity by integrating
1114 choice utility and outcome evaluation. *J Neurosci* **29**, 11020-11028 (2009).

1115 46. O'Callaghan, C., Vaghi, M.M., Brummerloh, B., Cardinal, R.N. & Robbins, T.W.
1116 Impaired awareness of action-outcome contingency and causality during healthy ageing and
1117 following ventromedial prefrontal cortex lesions. *Neuropsychologia* **128**, 282-289 (2019).

1118 47. Jobson, D.D., Hase, Y., Clarkson, A.N. & Kalaria, R.N. The role of the medial
1119 prefrontal cortex in cognition, ageing and dementia. *Brain Commun* **3**, fcab125 (2021).

1120 48. Cabeza, R., *et al.* Publisher Correction: Maintenance, reserve and compensation: the
1121 cognitive neuroscience of healthy ageing. *Nat Rev Neurosci* **19**, 772 (2018).

1122 49. Stern, Y. Cognitive reserve in ageing and Alzheimer's disease. *Lancet Neurol* **11**,
1123 1006-1012 (2012).

1124 50. Wook Yoo, S., *et al.* A Network Flow-based Analysis of Cognitive Reserve in
1125 Normal Ageing and Alzheimer's Disease. *Sci Rep* **5**, 10057 (2015).

1126 51. Wasano, K., Kaga, K. & Ogawa, K. Patterns of hearing changes in women and men
1127 from denarians to nonagenarians. *Lancet Reg Health West Pac* **9**, 100131 (2021).

1128 52. Peacock, J. & Peacock, P. *Oxford handbook of medical statistics* (Oxford university
1129 press, 2011).

1130 53. Taulu, S. & Simola, J. Spatiotemporal signal space separation method for rejecting
1131 nearby interference in MEG measurements. *Phys Med Biol* **51**, 1759-1768 (2006).

1132 54. Woolrich, M., Hunt, L., Groves, A. & Barnes, G. MEG beamforming using Bayesian
1133 PCA for adaptive data covariance matrix regularization. *Neuroimage* **57**, 1466-1479 (2011).

1134 55. Oostenveld, R., Fries, P., Maris, E. & Schoffelen, J.-M. FieldTrip: open source
1135 software for advanced analysis of MEG, EEG, and invasive electrophysiological data.
1136 *Computational intelligence and neuroscience* **2011**, 1-9 (2011).

1137 56. Woolrich, M.W., *et al.* Bayesian analysis of neuroimaging data in FSL. *Neuroimage*
1138 **45**, S173-S186 (2009).

1139 57. Penny, W.D., Friston, K.J., Ashburner, J.T., Kiebel, S.J. & Nichols, T.E. *Statistical*
1140 *parametric mapping: the analysis of functional brain images* (Elsevier, 2011).

1141 58. Mantini, D., *et al.* A signal-processing pipeline for magnetoencephalography resting-
1142 state networks. *Brain Connect* **1**, 49-59 (2011).

1143 59. Gross, J., *et al.* Good practice for conducting and reporting MEG research.
1144 *Neuroimage* **65**, 349-363 (2013).

1145 60. Hari, R., *et al.* IFCN-endorsed practical guidelines for clinical
1146 magnetoencephalography (MEG). *Clin Neurophysiol* **129**, 1720-1747 (2018).

1147 61. Nolte, G. The magnetic lead field theorem in the quasi-static approximation and its
1148 use for magnetoencephalography forward calculation in realistic volume conductors. *Phys*
1149 *Med Biol* **48**, 3637-3652 (2003).

1150 62. Huang, M., Mosher, J.C. & Leahy, R. A sensor-weighted overlapping-sphere head
1151 model and exhaustive head model comparison for MEG. *Physics in Medicine & Biology* **44**,
1152 423 (1999).

1153 63. Huang, M.X., *et al.* Commonalities and differences among vectorized beamformers in
1154 electromagnetic source imaging. *Brain topography* **16**, 139-158 (2004).

1155 64. Luckhoo, H.T., Brookes, M.J. & Woolrich, M.W. Multi-session statistics on
1156 beamformed MEG data. *Neuroimage* **95**, 330-335 (2014).

1157 65. Ramachandran, K.M. & Tsokos, C.P. *Mathematical statistics with applications in R*
1158 (Academic Press, 2020).

1159